The Impact of Channel Estimation Error on Space-Time Block and Trellis Codes in Flat and Frequency Selective Channels

Xuan Chi

Thesis submitted to the Faculty of the

Virginia Polytechnic Institute and State University

in partial fulfillment of the requirements for the degree of

Master of Science

in

Electrical Engineering

R. Michael Buehrer, Chair

Brian D. Woerner

Annamalai Annamalai

Dec 19, 2002

Blacksburg, Virginia

Keywords: Space-Time coding, Diversity, Channel estimation, Flat and frequency selective fading, Rayleigh Fading, MIMO, Maximal Ratio Combining, Trellis Coding.

Copyright 2003, Xuan Chi

The Impact of Channel Estimation Error on Space-Time Block and Trellis Codes in Flat and Frequency Selective Channels

Xuan Chi

(ABSTRACT)

Recently multiple antenna systems have received significant attention from researchers as a means to improve the energy and spectral efficiency of wireless systems. Among many classes of schemes, Space-Time Block codes (STBC) and Space-Time Trellis codes (STTC) have been the subject of many investigations. Both techniques provide a means for combatting the effects of multipath fading without adding much complexity to the receiver. This is especially useful in the downlink of wireless systems. In this thesis we investigate the impact of channel estimation error on the performance of both STBC and STTC. Channel estimation is especially important to consider in multiple antenna systems since (A) for coherent systems there are more channels to estimate due to multiple antennas and (B) the decoupling of data streams relies on correct channel estimation. The latter effect is due to the intentional cross-talk introduced into STBC.

ACKNOWLEDGEMENTS

I would like to express my gratitude to the ECE department of Virginia Tech and MPRG, especially to Dr. Buehrer for providing the opportunity to continue my graduate studies in the communication area.

I am deeply thankful to my advisor Dr. Buehrer for his great instruction on my study and thesis work. His broad knowledge in this area, insight into the problem and serious attitude towards research benefited me a lot. Thanks also is given to Dr. Woerner and Dr. Annamalai, as they solved some questions and some concepts. At same time, I would like to express my thanks to Jing Jiang and Nishant Kumar for their sincere help and valuable suggestions on my work.

Finally, on a personal note, I would like to thank my family; my wife, Zhongxin Li, who has supported me with encouragement and love, and my parents, Guizhi Ma and Hongzhi Chi, who invested their whole life in loving, caring and educating me, and to whom I dedicate this thesis. Their love has been an important source for my pursuing ideal of career, ideal of life.

Contents

1 Introduction **1**

1.1 Broadband Wireless Access 2

1.2 Evolution of Telecommunication Systems 3

1.3 Mobile Radio Propagation Environment 4

1.3.1 Multipath Channels 5

1.3.2 Rayleigh & Ricean Fading 6

1.3.3 Frequency Selective Fading 8

1.3.4 Doppler Shift 10

1.4 ISI cancellation 11

1.4.1 ISI Channel Representation 11

1.4.2 Linear Equalizer 12

1.5 Mathematical Notation 15

1.6 Scope of thesis 16

2 Space Time Processing and The MIMO Channel 18

2.1 MIMO Channel 19

2.1.1 Capacity of MIMO Channels 20

2.2 Spatial Diversity Performance Analysis 26

2.2.1 Receiver Diversity 27

2.2.2 Selection Combining (SC) 28

2.2.3 Maximum Ratio Combining (MRC) 29

2.2.4 Equal Gain Combining (EGC) 32

2.3 Discussion 33

3 Impact of Channel Estimation Error on STBC 34

3.1 A simple review of STBC 35

3.1.1 Classical Diversity 36

3.1.2 Alamouti Scheme for 2Tx1Rx and 2Tx2Rx 37

3.1.3 Space-Time Block Coding Scheme Review 40

3.1.4 Orthogonal Designs 41

3.2 Impact of Channel Estimation Error 45

3.2.1 General Case 46

3.2.2 Case Study : 8Tx1Rx; 2Tx1Rx and 4Tx1Rx 49

3.2.3 Performance analysis for pilot power 57

3.3 Frequency Selective Fading 62

3.3.1 Frequency selective fading model and Implementation in Simulation 63

3.4 Discussion 64

4 The Impact of Channel Estimation Error on STTC 69

4.1 Introduction 69

4.2 Trellis Coded Modulation 70

4.2.1 TCM Encoding 71

4.2.2 TCM decoding 72

4.3 Space-Time Trellis Codes 74

4.3.1 Code Construction 75

4.3.2 Code Design 77

4.3.3 STTC Generator Matrix 77

4.3.4 STTC Transmitter and Receiver models 79

4.4 STTC performance 82

4.5 Simulation results 83

4.6 Conclusions 87

5 Conclusions and future work **89**

5.1 Conclusion 89

5.2 Future work 90

List of Figures

1.1 Typical Three-ray Rayleigh Fading Envelop at 900MHz 7

1.2 Rayleigh Distribution 8

1.3 Model of Digital Signaling on an ISI channel 12

1.4 Linear Transversal Equalizer with N Taps 13

2.1 Shannon Bound 23

2.2 MIMO Capacity as a function of SNR for (n_T, n_R)=(2,2)[15] 25

2.3 Diversity System Block 27

2.4 Diversity Receiver 28

2.5 BER for Selection Combining and Coherent BPSK Signaling in Rayleigh Fading 29

2.6 Metric Computer for Maximal Ratio Combining 31

2.7 BER for Maximal Ratio Combining and Coherent BPSK Signaling 32

2.8 BER for Equal Gain Combining 33

3.1 Receiver Diversity Performance Comparison 35

3.2 Classical Two Branch Diversity [13] 36

3.3 Almouti Code Model. Copy from [13] 38

3.4 BER Performance Comparison between 1Tx2Rx, 2Tx1Rx with 2Tx2Rx in Rayleigh fading 39

3.5 MIMO Simple Block Model 40

3.6 8 Transmit Antennas by 1 receive Antenna Model 50

3.7 M-Matrix 8Tx1Rx 53

3.8 Simulation results and theoretical Value for 8Tx1Rx STBC Flat Fading channel 55

3.9 M-Matrix 2Tx1Rx 56

3.10 Simulation results and theoretical Value for 2Tx1Rx STBC Flat Fading channel 57

3.11 M-Matrix 4Tx1Rx 58

3.12 Effect of Channel Estimation on 8Tx and 1Rx STBC 59

3.13 Theoretical Results, M-matrix results for 8Tx1Rx, 2Tx1Rx [18] 60

3.14 Fixed Length Pilot (1/5 Training Code) Data Results 61

3.15 Fixed Length Pilot (9/10 Training Code) Data Results 62

3.16 Two Ray Equal Power Frequency Selective Model 63

3.17 Frequency Selective Fading Channel Implementation 64

3.18 STBC's System Model 65

3.19 Two Tx with Two Rx Two Ray Equal Taps Frequency Selective Fading . . . 66

3.20 Effect of Channel Estimation on Eight Tx with One Rx Two Ray Equal Taps Frequency Selective Fading 67

3.21 Effect of Channel Estimation on 8Tx and 1Rx for two Ray 0.5/0.5 Tap Frequency Selective Fading 68

4.1 Encoder and signal mapping for the 4-state 8-PSK Ungerboeck trellis code . 72

4.2 Illustration of an error events 73

4.3 General structure of a trellis encoder 75

4.4 8PSK and QPSK signal sets 75

4.5 8PSK and QPSK signal sets 79

4.6 Base station transmitter with STTC and two antennas [11] 80

4.7 Mobile receiver with STTC and two receiver antennas [11] 81

4.8 Example of 2 Tx 4-state Trellis encoder 81

4.9 Error Bounds for 4 State STTC over Flat Rayleigh Fading Channel 84

4.10 Simulation Results for STTC Using Code of [26] 85

4.11 Simulation Results for STTC Using Code of [25] 86

4.12 Comparison STBC with STTC 87

4.13 Effect of Channel Estimation to STTC 88

List of Tables

1.1 Major mobile standards in North America 4

1.2 Major mobile standards in Europe 5

1.3 Typical Delay Spread 10

2.1 Main MIMO Techniques 20

3.1 Real Orthogonal Designs for STBC 41

3.2 Real Orthogonal Designs for STBC 43

4.1 4-PSK trellis codes for 2Tx by Tarokh[11] 78

4.2 4-PSK trellis codes for 2Tx from Baro [26] 78

4.3 4-PSK trellis codes 2Tx from Z. Chen.[25] 78

Chapter 1

Introduction

You see, wire telegraph is a kind of a very, very long cat. You pull his tail in New York and his head is meowing in Los Angeles. Do you understand this? And radio operates exactly the same way: you send signals here, they receive them there. The only difference is that there is no cat.

–Albert Einstein

The rapid growth in mobile communications has led to an increasing demand for high data rate communications services. Recent research in information theory has shown that large gains in the capacity and reliability of communications over wireless channels can be achieved by exploiting the spatial domain. One appealing technology called multiple input multiple output (MIMO), uses multiple antennas to both transmit and receive information, and

promises to achieve high spectral efficiency or improved energy efficiency.

1.1 Broadband Wireless Access

Broadband connectivity has been considered the future of the telecommunications industry for decades. It typically refers to those data services operating at data rates in excess of 1.544 Mbps (known as the T-1 rate) [1]. While the theoretical foundations of high data rate digital communications are apparently well-known [2], there has not been any practical solution to implement the massive amount of signal processing required to operate reliably over the poor quality "last-mile" channel. The principal obstacle to mass deployment of broadband data services is without any doubt the trade-off between performance and cost. In particular, the wireless terrestrial solution presents probably the most difficult technical challenges. Different users will have different needs: terminals may be mobile (moving while communicating), or fixed (static while communicating); moving speeds can be as high as those of a train; more than one channel may be required for a single user; bandwidth can be statically or dynamically assigned; communication between terminals can be direct or through base stations; and asynchronous transfer mode may be required. As a consequence of these requirements, wireless access has become an extremely important sector of telecommunications research[3].

1.2 Evolution of Telecommunication Systems

Most first generation wireless systems were introduced in the mid 1980's and can be characterized by the use of analog modulation techniques and the use of simple multiple access techniques such as Frequency Division Multiple Access (FDMA). Additionally, first generation telecommunications systems such as Advanced Mobile Phone Service (AMPS) [4] only provided voice communications. They also suffered from a low user capacity and security problems due to the simple radio interface used.

The second generation systems were introduced in the early 1990's and all use digital technology. This provided an increase in the user capacity of approximately three times. This was achieved in part by compressing the voice waveforms before transmission.

Third generation systems are an extension of the complexity of second generation systems. In the International Telecommunication Union (ITU), third generation networks are called International Mobile Telecommunications-2000 (IMT-2000), and in Europe, Universal Mobile Telecommunication System (UMTS). IMT-2000 provides a multitude of services including multimedia and high bit rate packet data. Wideband code division multiple access (WCDMA) has emerged as the primary air interface solution for third generation networks. Emerging requirements for higher data rate services and better spectrum efficiency are the main drivers identified for third generation mobile radio systems. The main objectives for the IMT-2000 air interface are:

- Full coverage and mobility for 144 Kbps, pedestrian 384 Kbps;

Cellular System	Year	type	Multiple Access	Channel BW	Generation
AMPS	1983	Analog	FDMA	30kHz	First
Narrowband AMPS	1992	Analog	FDMA	10kHz	First
U.S.Digital Cellular	1991	Digital	TDMA	30kHz	Second
IS-95	1993	Digital	CDMA	1.25MHz	Second
Wideband CDMA	2000	Digital	CDMA	5MHz	Third
cdma2000	2000	Digital	CDMA	1.25 MHz	Third

Table 1.1: Major mobile standards in North America

- Limited coverage and mobility for 2Mbps;
- High spectrum efficiency compared to existing systems;
- High flexibility for new services.

Table 1.1 and Table 1.2 [4] show some of the major cellular mobile phone standards in North America and Europe. One technology which is seen as a key to the next (fourth) generation systems is MIMO technology.

1.3 Mobile Radio Propagation Environment

In an ideal radio channel, the received signal would consist of only a single direct path signal, which would be a perfect replica of the transmitted signal. However in a real channel,

Cellular System	Year	type	Multiple Access	Channel BW	Generation
E-TACS	1985	Analog	FDMA	25kHz	First
NMT-900	1986	Analog	FDMA	12.5kHz	First
GSM	1990	Digital	TDMA	200kHz	Second
UMTS	2000	Digital	CDMA/TDMA	5MHz	Third

Table 1.2: Major mobile standards in Europe

the signal is modified during transmission. The received signal consists of a combination of attenuated, reflected, refracted, and diffracted replicas of the transmitted signal. The channel attenuates the signal as well, and can cause a shift in the carrier frequency if the transmitter or the receiver is moving (Doppler effect).

1.3.1 Multipath Channels

As stated, the RF signal from the transmitter may be reflected by objects such as hills, buildings, or vehicles, giving rise to multiple transmission paths at the receiver. The relative phase of these multiple reflected signals will be different causing constructive or destructive interference at the receiver. Furthermore, movement of the transmitter or receiver results in rapid variations in the envelope of the received signal, and is caused when plane waves arrive from many different directions with random phases and combine vectorially at the receive antenna. Typically, the received envelope can vary by as much as 30dB to 40dB over a fraction of a wavelength due to constructive and deconstructive interference [3]. Multipath

also causes time dispersion, because the multiple replicas of the transmitted signal propagate over different transmission paths, reaching the receiver antenna with different time delays. Time dispersion may require equalization in TDMA systems and Rake reception in CDMA systems if the dispersion is large enough.

1.3.2 Rayleigh & Ricean Fading

When the symbol duration is much greater than the time spread of the propagation path delay, all of the frequency components in the transmitted signal will experience the same random attenuation and phase shift due to multi-path fading. This introduces very little or no distortion into the received signal, and is termed frequency-nonselective, or flat fading. If there is no line-of-sight (LOS) component in the received signal (i.e., when the direct path is obstructed) as with propagation in an outdoor environment over a long distance, the received signal consists only of scattered components due to reflections. The overall amplitude of the signal that results from the addition of all components is modelled using a Rayleigh distribution and the phase is uniformly distributed on the interval of $[0, 2\pi]$. The distribution of a Rayleigh random variable is

$$p_z(x) = \frac{2x}{\Omega_p} \exp\left\{-\frac{x^2}{\Omega_p}\right\}^{1} \tag{1.1}$$

Figures 1.1 and 1.2 illustrate the envelope in time and the probability distribution of the envelope that occurs due to Rayleigh fading. If there is a direct LOS component in the

[1] Ω_p is the total received envelope power

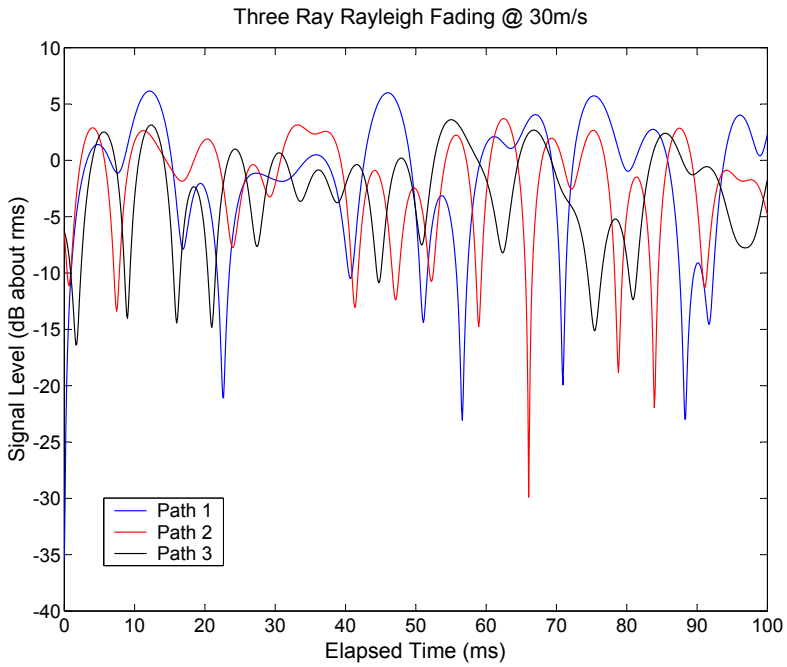

Figure 1.1: Typical Three-ray Rayleigh Fading Envelop at 900MHz

received signal along with scattered scattered components due to reflections, Ricean fading results. The resulting envelope of the received signal follows a Ricean distribution defined as:

$$p_z(x) = \frac{x}{\sigma^2} \exp\left\{-\frac{x^2+s^2}{2\sigma^2}\right\} I_0(\frac{xs}{\sigma^2}), x \geq 0 \tag{1.2}$$

where $I_0(\cdot)$ is the modified Bessel function of the first kinf and zero-order, σ^2 is variance of the multipath, and

$$s^2 = s^2 \cos^2(2\pi f_m cos\theta_0 t + \phi_0) + s^2 \sin^2(2\pi f_m sin\theta_0 t + \phi 0) \tag{1.3}$$

where $f_m cos\theta_0$ and ϕ_0 are the Doppler shift and random phase offset associated with the LOS or specular component, respectively [3]. The Ricean distribution is often described in

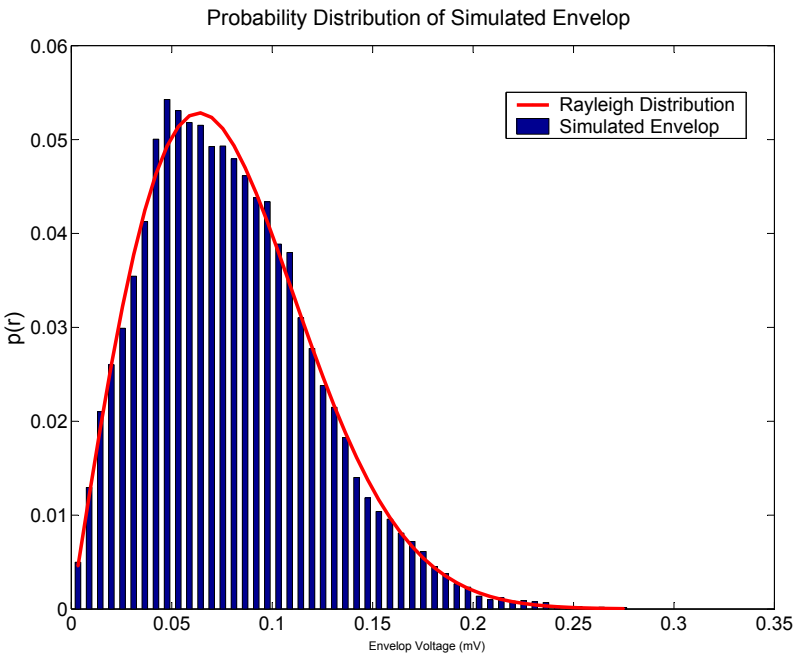

Figure 1.2: Rayleigh Distribution

terms of the parameter K which is defined as the ratio between the deterministic signal power and the variance of the multipath. It is given by $K = s^2/2\sigma^2$[5]

1.3.3 Frequency Selective Fading

In radio transmission when the propagation path delay spread is large compared to the inverse signal bandwidth, the frequency components in the transmitted signal will experience different phase shifts and attenuations, which is called frequency-selective fading. As the differential path delays become larger, even closely separated frequencies in the transmitted signal can experience significantly different attenuations and phase shifts [3]. Since the chan-

nel spectral response is not flat, it has dips or fades in the response due to reflections causing cancellation of certain frequencies at the receiver. This frequency selective attenuation leads to significant distortion in the received signal. This can be partly overcome in three ways.

- By transmitting a spread spectrum signal as in CDMA, any dips in the spectrum only result in a small loss of signal power, rather than a complete loss. Frequency selective fading is then combatted the use of a Rake receiver if the multipaths are resolvable.
- Another method is to split the transmission up into many small bandwidth carriers, as is done in a Orthogonal Frequency Division Multiplexing or OFDM transmission. The original signal is spread over a wide bandwidth thus, any nulls in the spectrum are unlikely to occur at all of the carrier frequencies. This will result in only some of the carriers being lost, rather than the entire signal. The information in the lost carriers can be recovered provided enough forward error correction is used.
- Thirdly, one can use an equalizer.
- Fourthly, narrow beam antennas can be used.

In a digital system, large delay spread leads to inter-symbol interference. This is due to the delayed multipath signal overlapping with the following symbols. This can cause significant errors in high bit rate systems, especially when using time division multiplexing (TDMA). As the transmitted bit rate is increased, the amount of inter-symbol interference (ISI) also increases. The effect starts to become very significant when the delay spread is greater than

50% of the bit time.

Table 1.3.3 [4] shows the typical delay spreads that can occur in various environments. The maximum delay spread in an outdoor environment is approximately 20μsec, thus significant intersymbol interference can occur at bit rates as low as 25kbps.

Environment or cause	Delay Spread	Maximum Path Length Difference
Indoor (room)	40nsec - 200nsec	12m - 60 m
Outdoor	1μsec - 20μsec	300m - 6km

Table 1.3: Typical Delay Spread

1.3.4 Doppler Shift

When a wave source and a receiver are moving relative to one another the frequency of the received signal will not be the same as the transmitted signal. When they are moving toward each other, the frequency of the received signal is higher than the source, and when they are moving away from each other, the frequency decreases. This is called the Doppler effect. Small Doppler spreads imply a large coherence time or a slowly changing channel. This effect becomes important when developing mobile radio systems. The amount the frequency of an individual received signal changes due to the Doppler effect depends on the relative motion between the source and receiver and on the speed of travel. The Doppler shift in frequency can be written as:

$$f_{D,n}(t) = f_m \cos\theta_n Hz \tag{1.4}$$

where $f_m = v/\lambda_c$ is the maximum Doppler shift, λ_c is the wavelength of the arriving plane wave, and θ_n is angle-of-arrival (or departure) of the nth received signal relative to the direction of movement. The maximum Doppler shift is also equal to the Doppler spread since θ_n is typically uniformly distributed on $[0, 2\pi]$.

1.4 ISI cancellation

Lucky [6] was the first to propose an adaptive (linear) equalizer for digital communication systems in the mid-1960s. This famous equalizer is called a "zero-forcing (ZF) equalizer". Soon after, Prokis and Miller [7] and Lucky [8] developed the linear LMS equalizer, based on the least mean square criterion. The LMS equalizer is more robust than the ZF equalizer, because it incorporates the effects of noise[3].

1.4.1 ISI Channel Representation

As is well known, the complex envelope of any pulse amplitude modulated signal can be expressed in the general form

$$\tilde{s} = A \sum_n b(t, \mathbf{x}_n) \tag{1.5}$$

where the A is the amplitude, $b(t, \mathbf{x}_n) = x_n h_a(t)$, $h_a(t)$ is the amplitude shaping pulse, and x_n is the symbol sequence. Suppose the time delay yields the symbol duration T. From

Figure 1.3 the signal after the channel can be expressed as

$$\begin{aligned} y_k = y(kT) &= \sum_n x_n f(kT - nT) + n(kT) \\ &\equiv \sum_n x_n f_{k-n} + n_k \\ &= x_k f_0 + \sum_{n \neq k} x_n f_{k-n} + n_k \end{aligned} \tag{1.6}$$

where $f_n = f(nT)$ is channel and n_k is noise. The first term in equation (1.6) is the desired

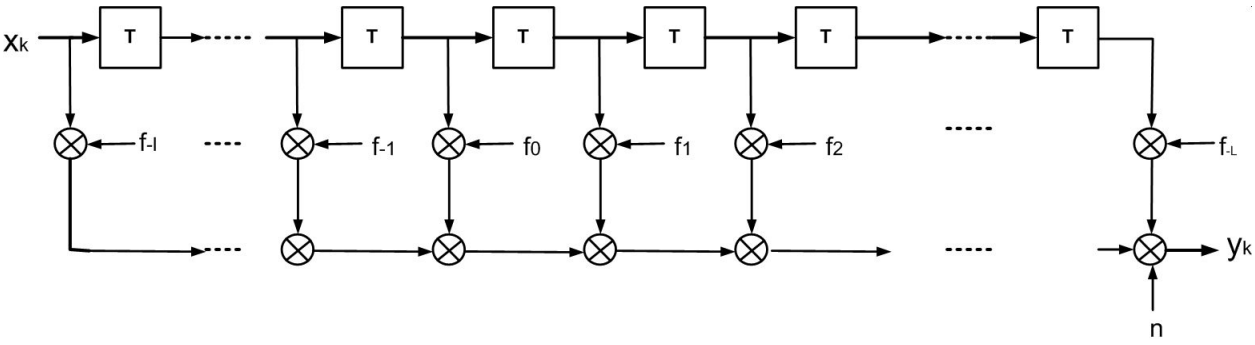

Figure 1.3: Model of Digital Signaling on an ISI channel

term, the second term is ISI, and the last term is the noise at the output of the matched filter.

1.4.2 Linear Equalizer

There are two kinds of linear equalizers, namely the Zero forcing (ZF) equalizer and Minimum Mean-Square-Error (MMSE) equalizer. Normally, they both can cancel the echoes, but MMSE is better than ZF in a channel with moderate to high SNR.

First, the desired equalizer's model is introduced at the Figure 1.4. The tap co-efficients of

the equalizer are denoted by the column vector

$$\mathbf{c} = [c_0, c_1, ..., c_{N-1}]^T \tag{1.7}$$

where N is the number of equalizer taps. Suppose the feed sequence of the equalizer is v_n,

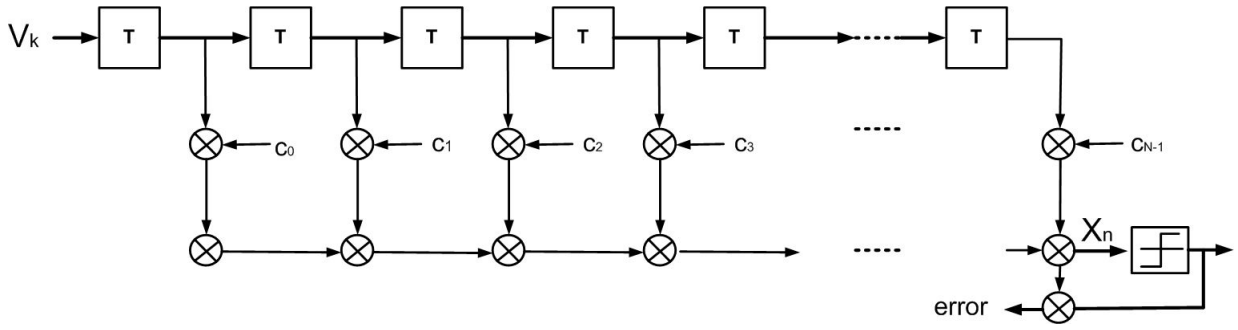

Figure 1.4: Linear Transversal Equalizer with N Taps

from Figure 1.4, the output of the equalizer is

$$\tilde{x}_n = \sum_{j=0}^{N-1} c_j v_{n-j} \tag{1.8}$$

where the $v_n = \sum_{n=0}^{L} h_n x_{k-n} + \eta_k$. The equalizer's impulse response can be represented as

$$\mathbf{q} = (q_0, q_1, ..., q_{N+L-1})^T \tag{1.9}$$

where

$$\begin{aligned} q_n &= \sum_{j=0}^{N-1} c_j h_{n-j} \\ &= \mathbf{c}^T \mathbf{h}(n) \end{aligned} \tag{1.10}$$

where

$$\mathbf{h}(n) = (h_n, h_{n-1}, ..., h_{n-N+1})^T \tag{1.11}$$

If the number of taps is an even value, perfect equalization means that

$$\mathbf{q} = \mathbf{e}_d = (0, 0, .., 1, 0, ..., 0)^T \tag{1.12}$$

Zero-Forcing Equalizer

To build this kind of equalizer, we wish to minimize the quantity $|q_n - \hat{q}_n|$ where $\hat{q}$ is the desired equalized channel. To accomplish this, we force the channel to $\tilde{\mathbf{q}} = (0, 0, .., 0, 1, 0, .., 0)$, hence the name 'Zero-Forcing equalizer'. For building the filter, the tap co-efficients must be known. Suppose the channel impulse response G is known, then the tap gain can be derived from Equation 1.12 as

$$\mathbf{c}_{op} = (\mathbf{H}^{-1})^T \tilde{q} \tag{1.13}$$

MMSE equalizer

The MMSE equalizer is more robust than the ZF equalizer in its performance and convergence properties [9] [10]. The basic idea of the MMSE is that it adjusts the tap coefficients to minimize the mean square error defined as

$$\begin{aligned} J &= E[|x_{n-d} - \tilde{x}_n|^2] \\ &= E[\mathbf{c}^T \mathbf{v}_n \mathbf{v}_n^H \mathbf{c}^* - 2Re(\mathbf{v}_n^H \mathbf{c}^* x_{n-d}) + |x_{n-d}|^2] \end{aligned} \tag{1.14}$$

The equalizer taps can be obtained by direct solution from

$$\mathbf{c}_{op} = (\mathbf{M}_v^T)^{-1} \mathbf{v}_x^* \tag{1.15}$$

where

$$\mathbf{M}_v = E|\mathbf{v}_n \mathbf{v}_n^H|$$

$$\mathbf{v}_x^H = E|\mathbf{v}_n^H x_{n-d}|$$

Adaptive Issues

In practice, the channel impulse response usually is not known. Thus, in order to obtain the tap coefficients we typically use an adaptive algorithm which usually exploits a training sequence. The most common adaptive algorithm is the LMS algorithm defined as [3]:

$$c_j^{n+1} = c_j^n + \alpha \varepsilon_n x_{n-j-d}^*, j = 0, ..., N-1 \tag{1.16}$$

where

$$\begin{aligned} \epsilon_n &= x_{n-d} - \tilde{x}_n \\ &= x_{n-d} - \textstyle\sum_{i=0}^{N-1} c_j v_{n-i} \end{aligned}$$

and x_n is the expected data. As stated this is typically known by using a training sequence followed by a decision directed model.

1.5 Mathematical Notation

In this paper vectors and matrices are written in boldface. For example, s is a scalar and $\mathbf{s}$ is a vector. $\mathbf{M}^T$, $\mathbf{v}^T$, $\mathbf{M}^H$, $\mathbf{v}^H$ designate transposition and Hermitian (complex conjugate

transposed) for matrices $\mathbf{M}$ and vector $\mathbf{v}$, respectively. Complex conjugation for scalars, matrices, and vectors is indicated as u^*, $\mathbf{M}^*$, $\mathbf{v}^*$, respectively, while notations $[\mathbf{M}]_{l,m}$ and $[\mathbf{v}]_k$ stand for the l,mth element of matrix $\mathbf{M}$ and the kth element of vector $\mathbf{v}$, respectively. We use the notation

$$\|\mathbf{v}\| = \sqrt{\sum_{i=1}^{M} |v_i|^2} \tag{1.17}$$

for the 2-norm of complex M-vector $\mathbf{v}=[v_1, ..., v_m]^T$, and $\mathbf{I}_M$ for the MxM identity matrix.

1.6 Scope of thesis

Readers of this thesis need to have knowledge of multiple disciplines within the communications area, so I attempt to cover the fundamental concepts and the general ideas which will be helpful to us. This thesis is only analytical in nature, but mathematical derivations are the basic tools to better learn how to develop effective products. All of the analysis in this thesis is based on pure theory without any hardware implementation being considered.

Chapter 1 begins with an overview that is intended to introduce a broad array of issues relating to wireless communications. Included is a description of various wireless systems and channel models (particularly Rayleigh fading and Ricean Fading). It then goes on to discuss frequency selective fading included ISI, and ISI cancellation schemes. Chapter 2 treats the Multiple Input Multiple Output (MIMO) channel and diversity. It begins with a discussion of the MIMO channel, and provides a spatial discussion of diversity performance. Chapter 3 is devoted to STBC and the impact of channel estimation error on STBC. The chapter begins

with simple review of STBC. It then goes on to discuss the general STBC case with a model for estimating the impact of channel estimation error on STBC, it conduces with examples which illustrate the impact of channel estimation error on STBC performance. Chapter 4 covers space-time trellis coding(STTC). The chapter begins with an overview of the trellis code modulation (TCM). This is followed by performance analysis of STTC including the impact of channel estimation error. Finally, the chapter wraps up with performance comparison between the STBC and STTC.

Chapter 2

Space Time Processing and The MIMO Channel

The wireless channel, unlike the Gaussian channel, suffers from attenuation due to the destructive addition of multipath. This time-varying attenuation makes it very difficult for the receiver to determine the transmitted signal unless some less-attenuated replica of the transmitted signal is also provided to the receiver. This technique is termed "diversity" and is the single most important contributor to reliable wireless communication in fading channels. Diversity can be obtained via space (using multiple antennas), time (using error correction codes) or frequency (using an equalizer). We focus on spatial diversity in this thesis. Spatial diversity has traditionally been accomplished by using multiple, widely spaced antennas at the receiver. This can be challenging in the downlink of a wireless system due to the limited size of the typical mobile receiver.

Recently, transmit diversity has been studied extensively as a method of combatting the detrimental effects in wireless fading channels because it allows for spatial diversity without adding antennas to the mobile receiver. Specifically, space-time coding has been proposed[11], which combines signal processing at the receiver with coding techniques at the transmitter appropriate to multiple transmit antennas to provide significant diversity benefit. Since this form of diversity does not require multiple receive antennas it is useful for downlink communications.

2.1 MIMO Channel

Space-Time Coding (STC) schemes combine channel code design and the use of multiple transmit antennas. The encoded data can be split into n_T streams that are simultaneously transmitted using n_T transmit antennas. This can provide improvement in the bandwidth efficiency of wireless systems provided $n_R > n_T$ receive antennas are employed at the receiver. Alternatively, redundant symbols can be sent over multiple antennas to obtain diversity advantage. The received signal is a linear superposition of these simultaneous symbols corrupted by noise and channel-induced ISI. Space-time decoding algorithms, as well as channel estimation techniques, are incorporated at the receiver in order to achieve both diversity advantage and coding gain.

Various techniques to exploit the capabilities of MIMO channels have been proposed in the literature. The genal classes of STC are listed in Table 2.1.

BLAST- Bell Labs Layered Space-Time Architecture	Foschini. al [12]
Space-Time Trellis Codes(STTC)	Tarokh [11]
Space-Time Block Codes(STBC)	Almouti [13]

Table 2.1: Main MIMO Techniques

2.1.1 Capacity of MIMO Channels

One of the most famous of all results in information theory is Shannon's channel coding theorem. For a given channel, there exists a code that will permit the error-free transmission across the channel at a rate R, provided $R < C$, the channel capacity. Equality is achieved only when the SNR is infinite. The Shannon-Hartley law states that the channel capacity of a band-limited Additive White Gaussian Noise(AWGN) channel can be expressed as

$$C = Wlog_2(1 + S/N) \qquad [bits/second] \tag{2.1}$$

where W is the channel bandwidth, C is the channel capacity in bits/sec, and S/N is the channel signal-to-noise ratio.

Channel Coding Theorem(CCT)

1. Its direct part says that for rate $R < C$ there exits a coding system with arbitrarily low error rates as we let codelength $N \to \infty$.

2. The converse part states that for $R \geq C$ the bit and block error rates are strictly bounded away from zero for any coding system.

Bandwidth Efficiency characterizes how efficiently a system uses its allotted bandwidth and is defined as

$$\eta = \frac{\textbf{Transmission Rate}}{\textbf{Channel bandwidth W}} \qquad [bits/s/Hz].$$

From it, we can calculate the *Shannon limit* as

$$\eta_{max} = log_2(1 + \tfrac{S}{N}) \qquad [bits/s/Hz].$$

Shannon Bound

Average Signal Power S can be expressed as

$$S = \frac{k\mathbf{E}_b}{T} = RE_b$$

where

- E_b is the energy per bit,
- k is the number of bits transmitted per symbol,
- T is the duration of a symbol,
- $R = k/T$ is the transmission rate of the system in bits/s,
- S/N is called the signal-to noise ratio , $N = N_0W$ is the total noise power and N_0 is the one-sided noise power spectral density

The bandwidth efficiency is then:

$$\eta_{max} = log_2(1 + \frac{RE_b}{N_0 W}). \tag{2.2}$$

This can be solved to obtain the minimum bit energy required for reliable transmission, called the **Shannon bound**:[1]

$$\frac{E_b}{N_0} \geq \frac{2^{\eta_{max}} - 1}{R/W} \tag{2.3}$$

Since $R/W = \eta_{max}$ is the limiting spectral efficiency, we obtain a bound from Equation (2.3) on the minimum bit energy required for reliable transmission at a given spectral efficiency:

$$\frac{E_b}{N_0} \geq \frac{2^{\eta_{max}} - 1}{\eta_{max}} \tag{2.4}$$

The result that comes from Equation (2.4) is shown in Figure 2.1 and compared to several modulation and coding schemes [14] From the Figure 2.1, we can find the $\frac{E_b}{N_0}$ starts from -1.59 dB, this is called the fundamental limit. For infinite amounts of bandwidth $C_c \longrightarrow 0$

$$\frac{E_b}{N_0} \geq \lim_{\eta_{max} \to 0} \frac{2^{\eta_{max}} - 1}{\eta_{max}} = ln(2) = -1.59dB \tag{2.5}$$

This is the absolute E_s/N_0 required to reliably transmit one bit of information and the reason why the SNR in Figure 2.1 starts from -1.5dB.

[1] In order to calculate η, we must suitably define the channel bandwidth W. One commonly used definition is the 99% bandwidth definition.i.e, W is defined such that 99% of the transmitted signal power falls within the band of width W

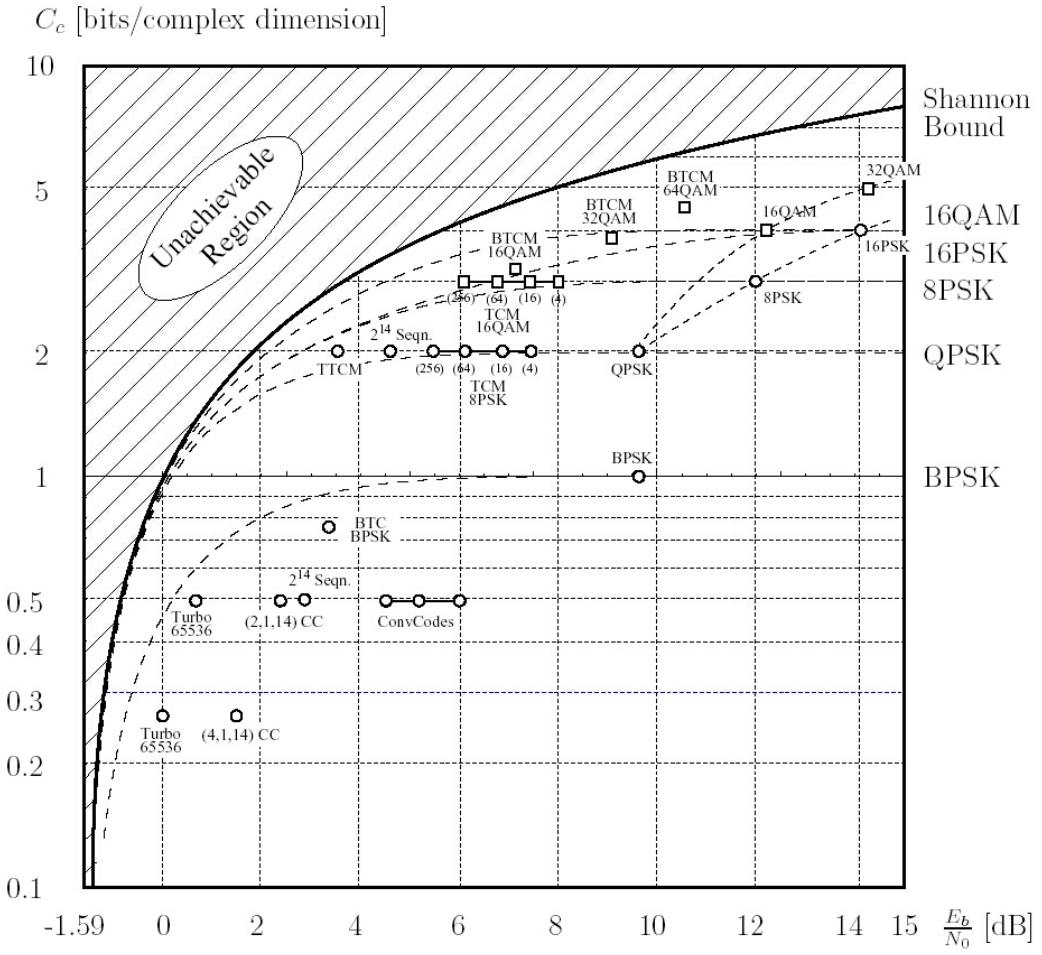

Figure 2.1: Shannon Bound

MIMO Capacity

A key result for the capacity of MIMO channels was obtained originally by Foschini and Gans in [12]. Assuming that the transmitted signal vector is composed of n_T statistically independent spatially separated equal power components each with a Gaussian distribution. The capacity is described by (see [12])

$$C = logdet[I_{n_R} + (SNR/n_T)H^{\dagger}H] \tag{2.6}$$

where $H^{\dagger}$ corresponds to the conjugate of H, $det(M) = \prod \lambda(M)$, $det(I+M) = \prod(1+\lambda(M))$ and I_{n_R} is an $n_R x n_R$ identity matrix. R. Gozali has derived the capacity of SISO, SIMO, MISO, and MIMO in his dissertation (see [15]). Here an outline is given.

• **Case Study I: Signal-Input Single-Output(SISO) Channel** In this case, a signal antenna channel is used at each side of the wireless link and thus H is a complex scalar.

$$C = log2(1 + SNR|H|^2) \tag{2.7}$$

where $|H|^2$ is the normalized channel power characteristic. In AWGN channel, $H = 1$. This is well known Shannon capacity formula.

• **Case Study II: Signal-Input Multiple-Output(MISO) Channel** Different results will be derived by using different combining schemes. For optimal combining, the capacity is

$$C = log_2 \left[1 + SNR \sum_{j=1}^{n_R} |H_j|^2\right] \tag{2.8}$$

and the capacity of SIMO using selection combining is

$$C = max_m log_2 \left[1 + SNR|H_m|^2\right] = log_2 \left[1 + SNR(max_m|H_m|^2)\right] \tag{2.9}$$

where $m \in 1, ..., n_r$.

• **Case Study III: Multiple-Input Signal-Output (MISO) Channel** The MISO channel can use transmit diversity. By applying n_T transmit antennas and a single receive antenna to Equation (2.6), the capacity of MISO is:

$$C = log_2 \left[1 + (SNR/n_T) \sum_{i=1}^{n_T} |H_i|^2\right] \tag{2.10}$$

• **Case Study IV: Multiple-Input Multiple-Output (MIMO) Channel** If assuming $n = n_T = n_R$, the MIMO capacity is

$$C = nlog_2(1 + (SNR/n)) \rightarrow SNR/ln(2) \;\; as \;\; n \rightarrow \infty \tag{2.11}$$

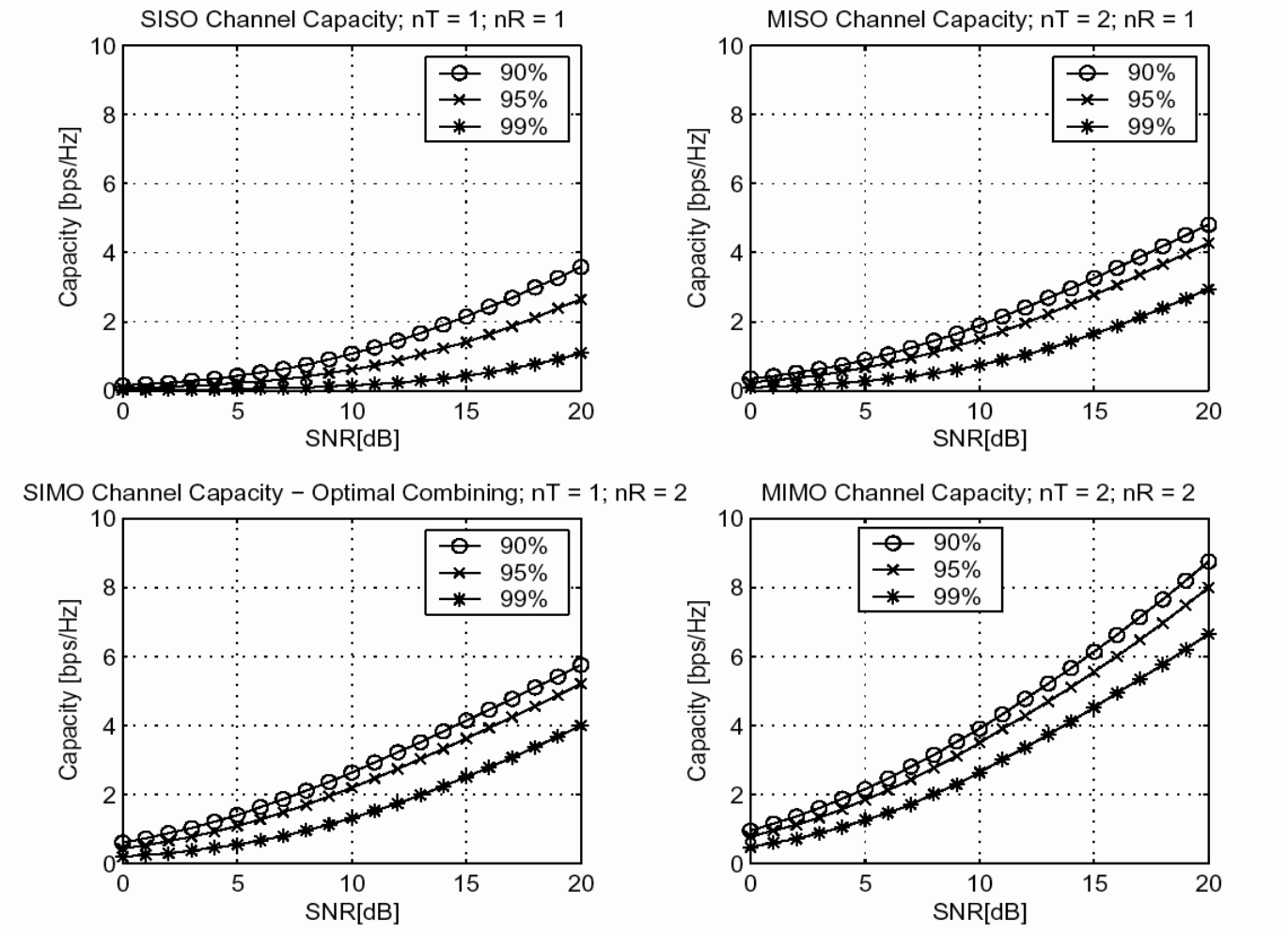

Figure 2.2: MIMO Capacity as a function of SNR for (n_T, n_R)=(2,2)[15]

2.2 Spatial Diversity Performance Analysis

In the previous section we showed that multiple antennas (ie MIMO channels) could be used for improving spectral efficiency. In this section we discuss another application of the MIMO channel, spatial diversity.

Transmit diversity uses multiple transmit antennas to provide the receiver with multiple uncorrelated replicas of the transmitted signal. The advantage is that the complexity of having multiple antennas is placed on the transmitter, which can be shared among many receivers for the downlink of a wireless system, while still providing diversity benefit.

Before we investigate transmit diversity we first explore the more traditional form of spatial diversity, receive diversity. For simplicity of notation, let $K = n_R$ (Number of receiver antennas) and $U = n_T$ (Number of transmitter antennas) and consider the system in Figure (2.3). Further we define

- A transmitted signal, $s(t)$;
- A received signal, $r(t)$;
- A channel, $h(t)$;
- An additive noise random process, $n(t)$;

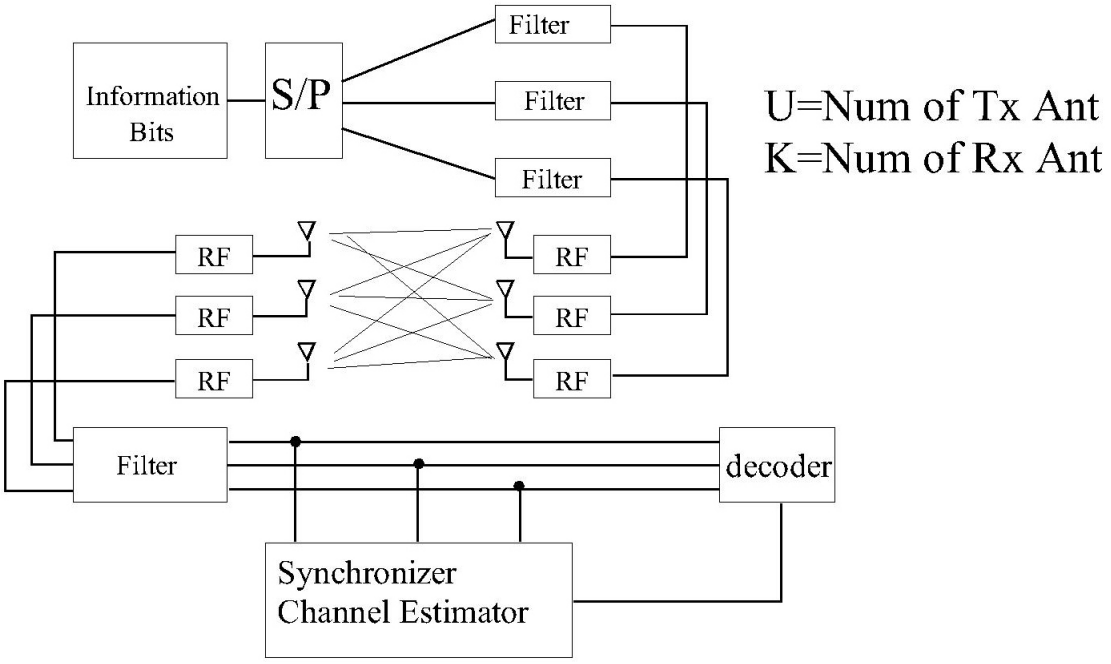

Figure 2.3: Diversity System Block

2.2.1 Receiver Diversity

When there is a single transmit antenna, but multiple receive antennas, we create $\hat{s}(t) = f(r_L(t))$ where the function $f(r_L(t))$ is a combining function as shown in Figure 2.4. There are many methods for combining the signals that are received on the disparate diversity branches. They are Selection Combining(SC), Equal Gain Combining (EGC), Switch Combining (SC) and Maximal Ratio Combining(MRC).

If the signal $\tilde{s}(t)$ is transmitted, the received complex envelopes (where $\tilde{(\bullet)}$ represents complex envelope) on the different diversity branches are

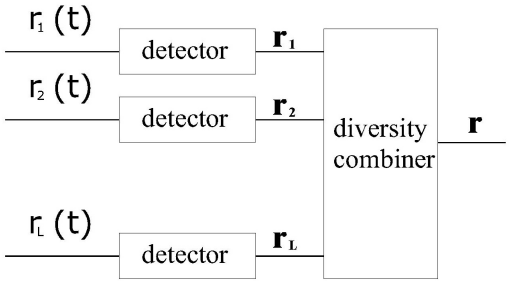

Figure 2.4: Diversity Receiver

$$\tilde{r}_k(t) = \tilde{h}_k \tilde{s}(t) + \tilde{n}_k(t), \qquad k = 1, ..., L \tag{2.12}$$

where $\tilde{h}_k = \alpha_k e^{-j\phi_k}$ is the fading gain associated with the k^{th} branch. The AWGN processes $\tilde{n}_k(t)$ are assumed to be independent from branch to branch. To simplify analysis, the diversity branches are usually assumed to be uncorrelated[2].

2.2.2 Selection Combining (SC)

With selection combining (SC), the branch yielding the highest signal-to-noise ratio is always selected. In this case, the diversity combiner in Figure 2.4 performs the operation

$$\tilde{r} = \max(|\tilde{r}_k|) \tag{2.13}$$

The bit error probability for selection combining in Rayleigh fading is plotted in Figure 2.5.

[2]Correlation will reduce the achievable diversity gain; therefore, the uncorrelated branch assumption gives optimistic results. Nevertheless,we have evaluated the performance of the various diversity combining techniques under the assumption of uncorrelated branches.

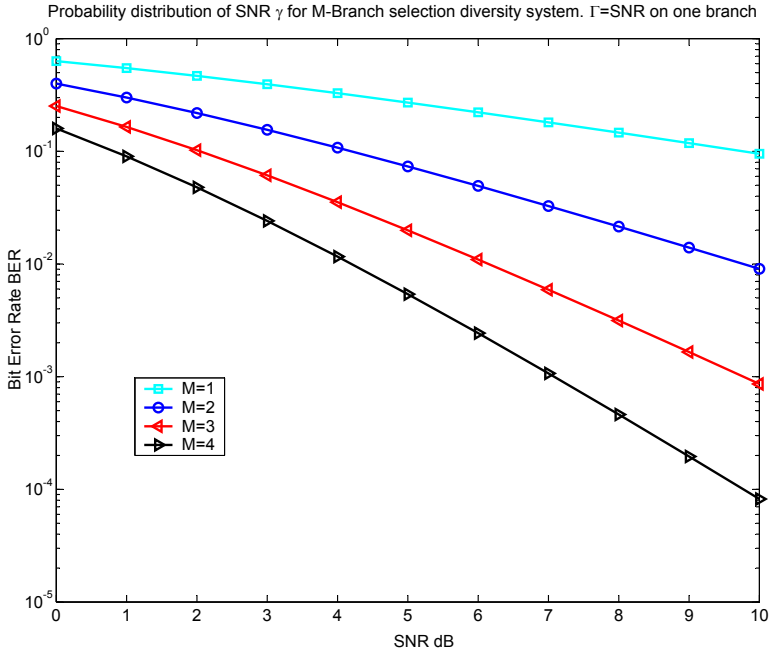

Figure 2.5: BER for Selection Combining and Coherent BPSK Signaling in Rayleigh Fading

2.2.3 Maximum Ratio Combining (MRC)

With maximal ratio combining (MRC), the diversity branches are weighted by their respective complex fading gains and then combined. MRC realizes maximal likelihood (ML) receiver as we now show. Referring to Equation (2.12), the vector

$$\tilde{r} = (\tilde{r}_1, \tilde{r}_2, ..., \tilde{r}_L) \tag{2.14}$$

has the multivariate Gaussian distribution

$$\begin{aligned} p(\tilde{r}|\mathrm{h}, \tilde{s}(t)) &= \prod_{k=1}^{L} \frac{1}{2\pi N_0} exp\{-\frac{1}{2N_0}|\tilde{r}_{k,i} - h_k\tilde{s}|^2\} \\ &= \frac{1}{(2\pi N_0)^{LN}} exp\{-\frac{1}{2N_0}\sum_{k=1}^{L}|\tilde{r}_k - h_k\tilde{s}|^2\} \end{aligned} \tag{2.15}$$

where h=$(h_1, h_2, ..., h_L)$ is the channel vector. From this expression, the ML receiver chooses the message vector $\tilde{\mathbf{s}}_m$ that maximizes the metric

$$\begin{aligned} \mu(\tilde{s}) &= -\sum_{k=1}^{L} |\tilde{r}_k - h_k \tilde{s}|^2 \\ &= -\sum_{k=1}^{L} \{|\tilde{r}_k|^2 - 2Re(h_k^* \tilde{r}_k, \tilde{s}) + |h_k|^2 |\tilde{s}|^2\}. \end{aligned} \tag{2.16}$$

Since $\sum_{k=1}^{L} |\tilde{r}_k|^2$ is independent of the hypothesis as to which $\tilde{\mathbf{s}}_m$ was sent and $|\tilde{\mathbf{s}}|^2 = 2E$, the receiver simply needs to maximize the metric:

$$\begin{aligned} \mu_2(|\tilde{s}|^2) &= \sum_{k=1}^{L} Re(h_k^* \tilde{r}_k, \tilde{s}_m) - E \sum_{k=1}^{L} |h_k|^2 \\ &= \sum_{k=1}^{L} Re(h_k^* \int_0^T \tilde{r}_k(t) \tilde{s}^*(t) dt) - E \sum_{k=1}^{L} |h_k|^2 \end{aligned} \tag{2.17}$$

If signals have equal energy then the last term can be cancelled, since it is the same as for all message vectors. This results in:

$$\begin{aligned} \mu_3(\tilde{s}) &= \sum_{k=1}^{L} Re(h_k^* \tilde{r}_k, \tilde{s}) \\ &= \sum_{k=1}^{L} Re\left(h_k^* \int_0^T \tilde{r_k}(t) \tilde{s}^*(t) dt \right) \end{aligned} \tag{2.18}$$

An alternative form of the ML receiver can also be obtained by rewriting the metric in Equation (2.17) as

$$\begin{aligned} \mu_4(\tilde{s}) &= Re(\sum_{k=1}^{L} h_k^* \tilde{r}_k, \tilde{s}) - E \sum_{k=1}^{L} |h_k|^2 \\ &= \int_0^T Re\{(\sum_{k=1}^{L} h_k^* \tilde{r_k(t)}) \tilde{s}^*\} dt - E \sum_{k=1}^{L} |h_k|^2 \end{aligned} \tag{2.19}$$

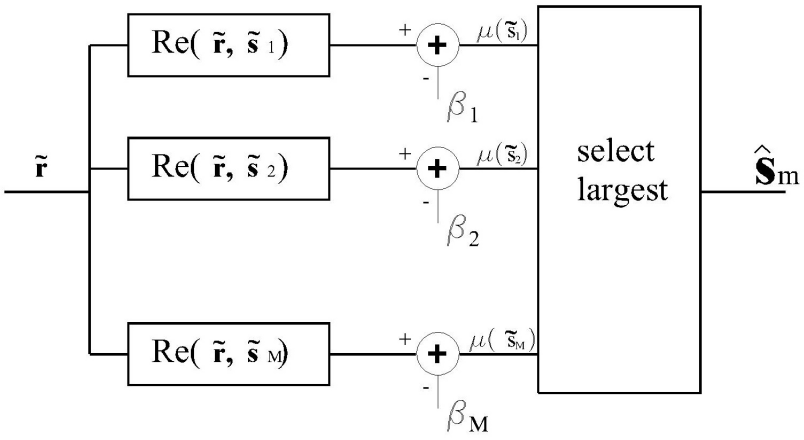

Figure 2.6: Metric Computer for Maximal Ratio Combining

From the above derivation, the ML receiver can be constructed. The diversity combiner in Figure 2.4 just generates the sum.

$$\tilde{r} = \sum_{k=1}^{L} h_k^* \tilde{r}_k \tag{2.20}$$

which is then applied to the metric computer shown in Figure 2.6, where β_m equals to $E_M \sum_{k=1}^{L} |\mathrm{h}_k^*|^2$. Since MRC is a coherent detection technique, it only works well for coherent signaling techniques, e.g., BPSK and M-QAM.

The MRC technique has been shown to be optimum if diversity branch signals are mutually uncorrelated and follow a Rayleigh distribution[16]. The bit error probability for maximal ratio combining is plot in Figure 2.7

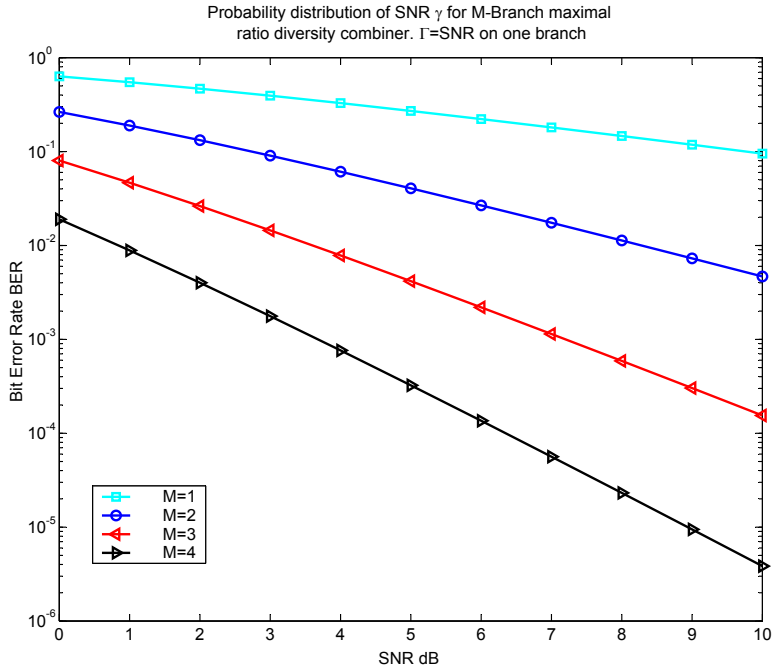

Figure 2.7: BER for Maximal Ratio Combining and Coherent BPSK Signaling

2.2.4 Equal Gain Combining (EGC)

Equal gain combining (EGC) is similar to MRC because the diversity branches are co-phased, but different from MRC in that the diversity branches are not weighted. In other words, $\tilde{r} = \sum_{k=1}^{L} e^{-j\phi_k} r_k$ In practice, such a scheme is useful for modulation techniques having equal symbols, e.g., M-PSK, and with signals of unequal energy. The bit error probability for equal gain combining is plot in Figure 2.8

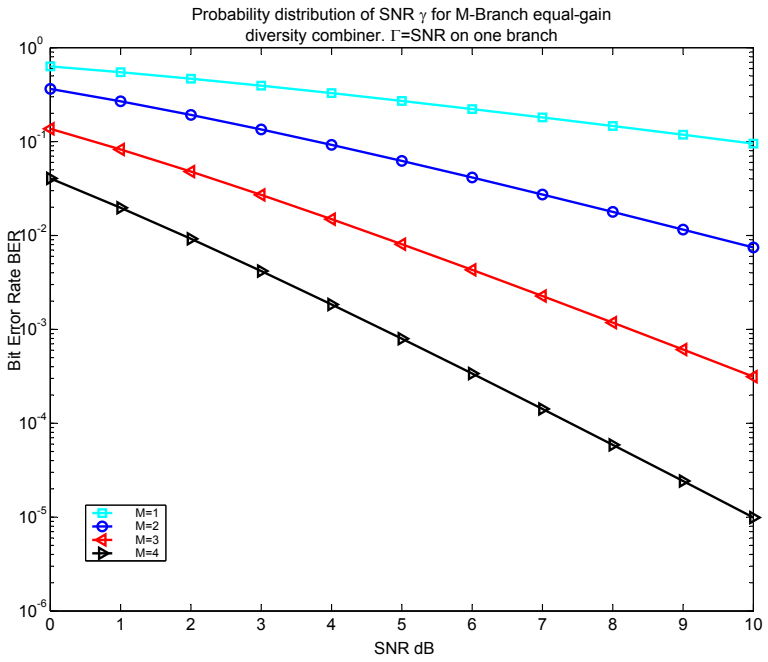

Figure 2.8: BER for Equal Gain Combining

2.3 Discussion

The MIMO channel can be exploited for improved spectral efficiency or energy efficiency. The traditional means of exploiting spatial channels is via recieve diversity. We have shown that by using multiple receive antennas we can dramatically improve the energy efficiency of wireless systems operating in Rayleigh fading. However, many applications do not permit many receive antennas. This leads us to other MIMO techniques, such as Space-Time Block Codes and Space-Time Trellis codes which can achieve spatial diversity without multiple receive antennas.

Chapter 3

Impact of Channel Estimation Error on STBC

We showed in Chapter 2 that receive diversity is an effective method to improve energy efficiency in the presence of Rayleigh fading. However, some applications do not permit multiple receive antennas. We thus would like to exploit the MIMO channel to achieve transmit diversity. Previously, various transmit diversity techniques have been published in the literature. In 1998, space-time coding was proposed in [11]. This technique combines signal processing at the receiver with a coding technique appropriate to multiple transmit antennas. The space-time decoding process at the receiver required trellis decoding (STTC) and may be highly complex for some applications. In addressing this issue, an effective and simple transmit diversity scheme was proposed by Alamouti [13] for two transmit antennas and two receivers in 1998. One year later, the technique was generalized and the concept of

Space-Time Block Codes were introduced by Tarkokh[17].

In the past several years, the performance of MIMO using Space-Time Block Codes has been extensively investigated. This thesis mainly makes an analysis of how much impact channel estimation error has on performance. The basic idea was generated from [18].

3.1 A simple review of STBC

Receive diversity provides significant benefits to performance in a Rayleigh fading environment as shown in Figure 3.1. However, there are applications where having multiple receive

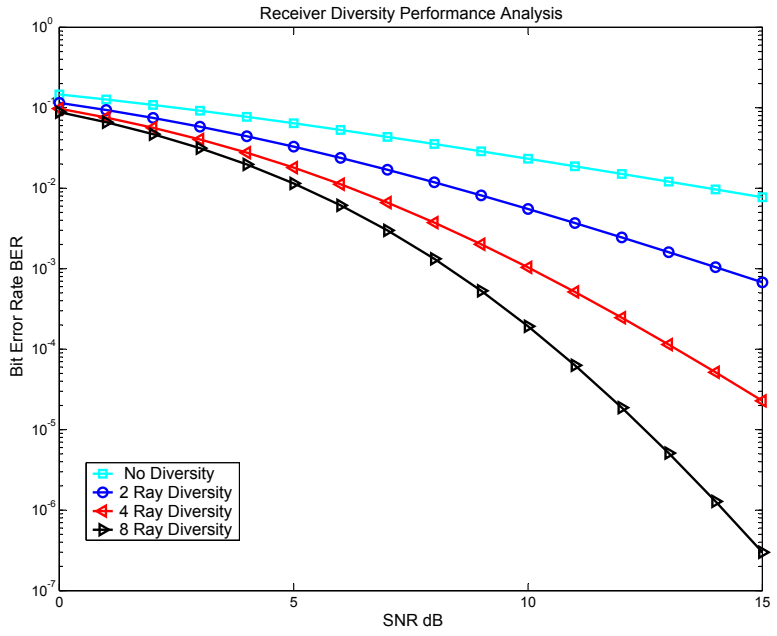

Figure 3.1: Receiver Diversity Performance Comparison

antennas is impractical. For example, in mobile systems the downlink does not lend itself well to receive diversity since the receivers are small and must be inexpensive. Thus, diversity techniques are needed which do not burden the receiver. One method of achieving spatial diversity without burdening the receiver is transmit diversity. One form of transmit diversity is space time block coding, which we will investigate in this section.

3.1.1 Classical Diversity

Consider the model shown in Figure. 3.2. We assume that h_0 and h_1 are uncorrelated and

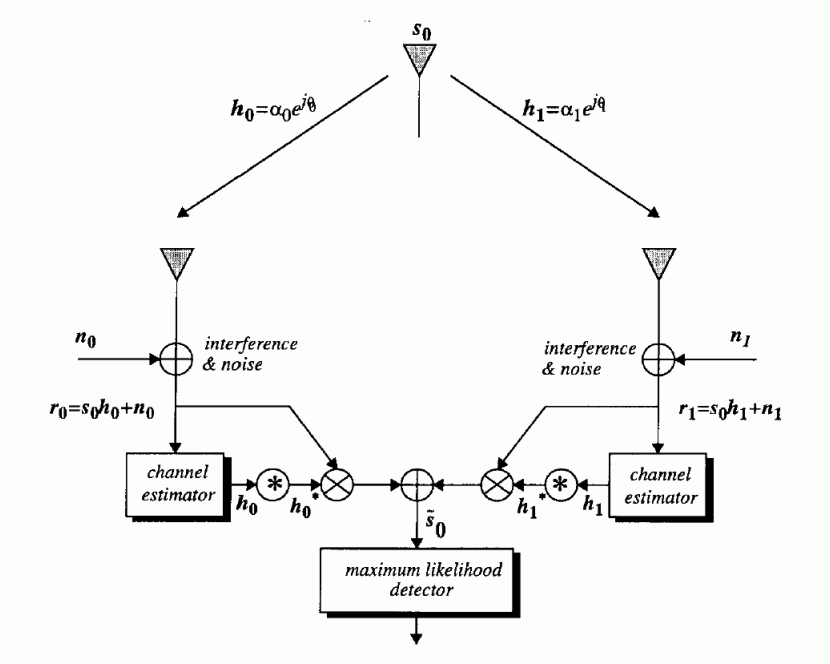

Figure 3.2: Classical Two Branch Diversity [13]

$$\begin{aligned} h_0 &= \alpha_0 e^{j\theta_0} \\ h_1 &= \alpha_1 e^{j\theta_1} \end{aligned} \tag{3.1}$$

where α_i is Rayleigh distributed and θ_i is uniformly distributed. Noise and interference are added at the two receivers. The resulting received baseband signals are

$$\begin{aligned} r_0 &= h_0 s_0 + n_0 \\ r_1 &= h_1 s_0 + n_1 \end{aligned} \tag{3.2}$$

where n_0 and n_1 are complex random Gaussian processes noise. Using MRC the decision statistic can be generated as :

$$\begin{aligned} \tilde{s}_0 &= \hat{h}_0^* \tilde{r}_0 + \hat{h}_1^* \tilde{r}_1 \\ &= h_0^*(h_0 s_0 + n_0) + h_1^*(h_1 s_0 + n_1) \\ &= (|h_0|^2 + |h_1|^2) s_0 + h_0^* n_0 + h_1^* n_1 \end{aligned} \tag{3.3}$$

where we have assumed perfect channel estimation ($\hat{h}_i$=h_i).

3.1.2 Alamouti Scheme for 2Tx1Rx and 2Tx2Rx

To introduce the idea of STBC, let us first consider Almouti's original scheme as shown in Figure 3.3. In this method, during time slot 1, the symbol s_0 is transmitted from antenna 0 and symbole s_1 was transmitted from antenna 1. During time slot 2 symbol $-s_1^*$ is transmitted on antenna 0 and s_0^* is transmitted on antenna 1. Thus, over 2 time slots, 2 symbols are transmitted (ie. the rate is 1). The received signal on the two receive antennas during

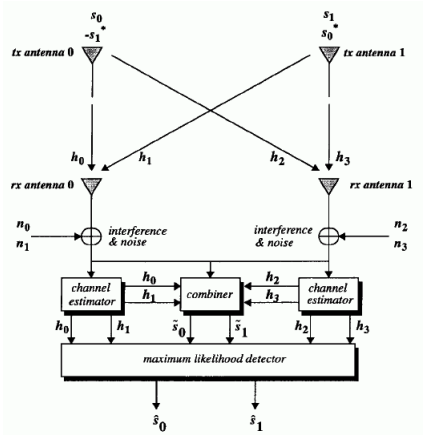

Figure 3.3: Almouti Code Model. Copy from [13]

the two time slots is

$$\begin{aligned} r_0 &= h_0 s_0 + h_1 s_1 + n_0 \\ r_1 &= -h_0 s_1^* + h_1 s_0^* + n_1 \\ r_2 &= h_2 s_0 + h_3 s_1 + n_2 \\ r_3 &= -h_2 s_1^* + h_3 h_3^* + n_3 \end{aligned} \tag{3.4}$$

where r_0 and r_2 are the received signals at time t on antenna 0 and 1, r_1 and r_3 are the received signals at time $t+T$ on antenna 0 and 1, and n_0, n_1, n_2 and n_3 are complex noise samples. If the MRC is used, the decision statistic will be

$$\begin{aligned} \tilde{s}_0 &= h_0^* r_0 + h_1 r_1^* + h_2^* r_2 + h_3 r_3^* \\ \tilde{s}_1 &= h_1^* r_0 - h_0 r_1^* + h_3^* r_2 - h_2 r_3^* \end{aligned} \tag{3.5}$$

Here, we assume the channel is perfectly known. The ML decision can be used to make a hard decision. Following the same rule, the decision statics for the case of two transmit

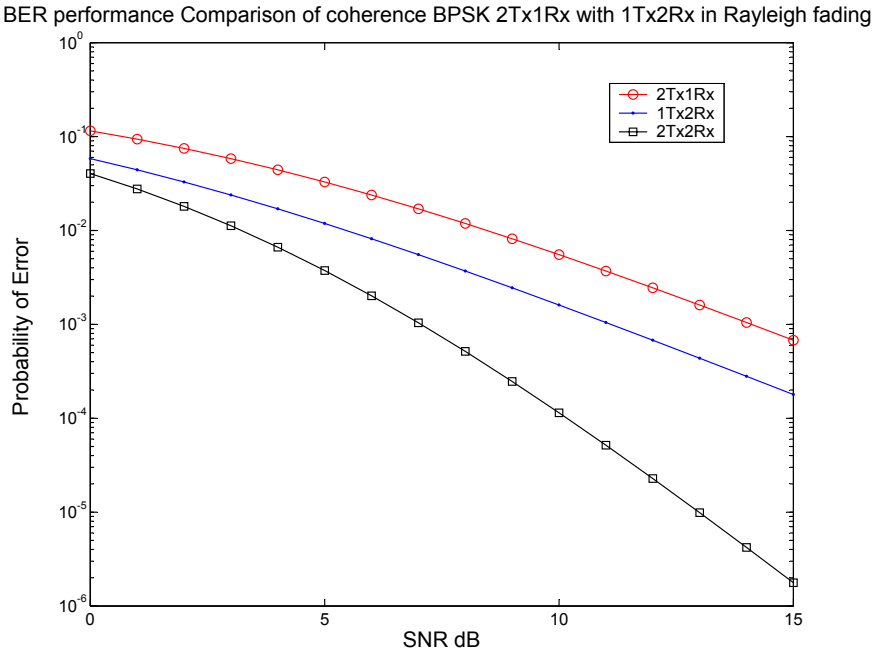

Figure 3.4: BER Performance Comparison between 1Tx2Rx, 2Tx1Rx with 2Tx2Rx in Rayleigh fading

antennas and one receiver antenna can be obtained as:

$$\begin{aligned} \tilde{s}_0 &= h_0^* r_0 + h_1 r_1^* \\ \tilde{s}_1 &= h_1^* r_0 - h_0 r_1^* \end{aligned} \tag{3.6}$$

The performance for the three cases is shown in Figure 3.4. From this results, 2Tx2Rx's performance is the best and 1Tx2Rx's performance is 3dB better than 2Tx1Rx's case. .

3.1.3 Space-Time Block Coding Scheme Review

The two antenna transmit diversity scheme described in section 3.1.2 is one example of a general technique known as Space Time Block Coding. Space Time Block Codes are special codes that provide diversity gain while maintaining orthogonality between code words after receiver processing. It maps a block of input symbols into space and time domains, creating an orthogonal sequence or a quasi-orthogonal sequence that will be transmitted from different transmit antennas. The receiver is composed of channel estimation, combining [1] and ML detection [2]. Because the transmitter antennas use the same frequency, there is no frequency penalty.The key to this technique is creating the space time orthogonal sequence while we will now discuss.

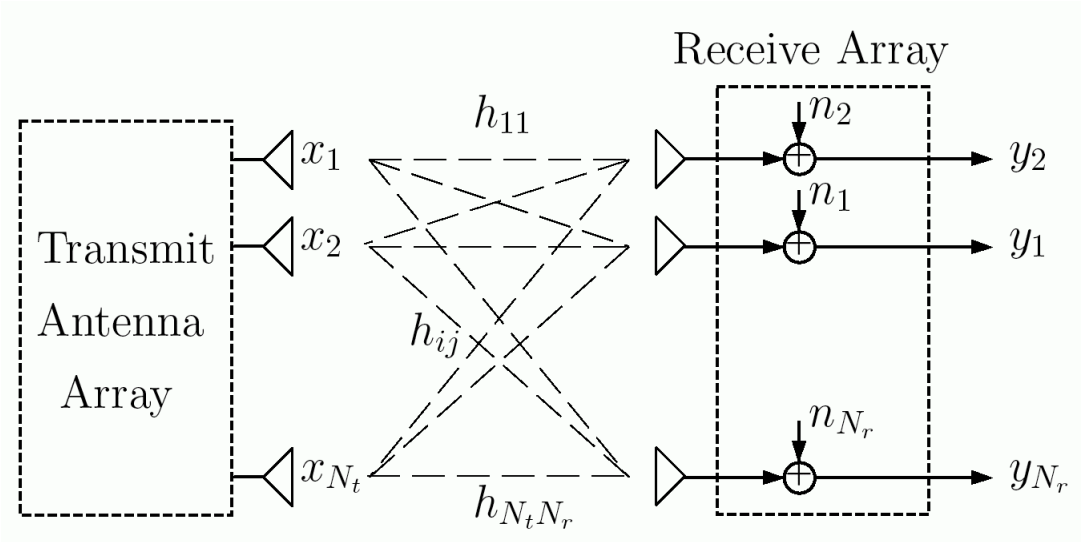

Figure 3.5: MIMO Simple Block Model

[1] Both Space domain and Time domain

[2] It is assumed that channel coherence time is greater than block length

Real Orthogonal Design	n_T	rate	input block length	output block length
G_2	2	1	2	2
G_4	4	1	4	4
G_8	8	1	8	8

Table 3.1: Real Orthogonal Designs for STBC

3.1.4 Orthogonal Designs

Space-Time block codes are based on the theory of orthogonal designs. There are two kinds orthogonal designs, real orthogonal designs and complex orthogonal designs.

Real Orthogonal Designs

A real orthogonal design of size n is an $n \times n$ orthogonal matrix with entries $\pm x_1, \pm x_2, ... \pm x_n$. Table 3.1 summarizes the characteristics of rate 1 real orthogonal designs, proposed originally in [11], for 2,4,8 transmit antennas. Note that real orthogonal designs of rate=1 do not exist for $n > 8$. We shall now describe the orthogonal designs of Table 3.1 by defining the specific code matrices.

- **Real Orthogonal Design I**: 2 transmit antennas r=1

$$G_2 = \begin{pmatrix} x_1 & x_2 \\ -x_2 & x_1 \end{pmatrix} \tag{3.7}$$

- **Real Orthogonal Design II**: 4 transmit antennas r=1

$$G_4 = \begin{pmatrix} x_1 & x_2 & x_3 & x_4 \\ -x_2 & x_1 & -x_4 & x_3 \\ -x_3 & x_4 & x_1 & -x_2 \\ -x_4 & -x_3 & x_2 & x_1 \end{pmatrix} \tag{3.8}$$

- **Real Orthogonal Design III**: 8 transmit antennas r=1

$$G_8 = \begin{pmatrix} x_1 & x_2 & x_3 & x_4 & x_5 & x_6 & x_7 & x_8 \\ -x_2 & x_1 & x_4 & -x_3 & x_6 & -x_5 & -x_8 & x_7 \\ -x_3 & -x_4 & x_1 & x_2 & x_7 & x_8 & -x_5 & -x_6 \\ -x_4 & x_3 & -x_2 & x_1 & x_8 & -x_7 & x_6 & -x_3 \\ -x_5 & -x_6 & -x_7 & -x_8 & x_1 & x_2 & x_3 & x_4 \\ -x_6 & x_5 & -x_8 & x_7 & -x_2 & x_1 & -x_4 & x_3 \\ -x_7 & x_8 & x_5 & -x_6 & -x_3 & x_4 & x_1 & -x_2 \\ -x_8 & -x_7 & x_6 & x_5 & -x_4 & -x_3 & x_2 & x_1 \end{pmatrix} \tag{3.9}$$

The code matrices G_2, G_4, and G_8 describe the symbols sent at each antenna (rows) during each symbol time (column). Note that the defining condition of an orthogonal design is that each column is orthogonal and $G_i^H G = I$

Complex Orthogonal Designs

We define a complex orthogonal design G_c of size n as an orthogonal matrix with entries $\pm x_1, \pm x_2, ... \pm x_n$,or their conjugates $\pm x_1^*, \pm x_2^*, ... \pm x_n^*$. Table 3.2 summarizes the charac-

Complex Orthogonal Design	n_T	rate	input block length	output block length
G_c^2	2	1	2	2
G_c^3	3	1/2	4	8
G_c^4	4	1/2	4	8
H_c^3	3	3/4	3	4
H_c^4	4	3/4	3	4

Table 3.2: Real Orthogonal Designs for STBC

teristics of few complex orthogonal designs, proposed originally in [11], for 2,3,4 transmit antenna. Note that unlike the real case, rate 1 designs exist only for $n = 2$. Following Table 3.2, the orthogonal transmission matrixes are described.

- **Complex Orthogonal Design I**: 2 transmit antennas r=1

$$G_c^2 = \begin{bmatrix} x_1 & x_2 \\ -x_2^* & x_1^* \end{bmatrix} \tag{3.10}$$

- **Complex Orthogonal Design II**: 3 transmit antennas r=1/2

$$G_c^3 = \begin{bmatrix} x_1 & x_2 & x_3 \\ -x_2 & x_1 & -x_4 \\ -x_3 & x_4 & x_1 \\ -x_4 & -x_3 & x_2 \\ x_1^* & x_2^* & x_3^* \\ -x_2^* & x_1^* & -x_4^* \\ -x_3^* & x_4^* & x_1^* \\ -x_4^* & -x_3^* & x_2* \end{bmatrix} \tag{3.11}$$

- **Complex Orthogonal Design III**: 4 transmit antennas r=1/2

$$G_c^4 = \begin{bmatrix} x_1 & x_2 & x_3 & x_4 \\ -x_2 & x_1 & -x_4 & x_3 \\ -x_3 & x_4 & x_1 & -x_2 \\ -x_4 & -x_3 & x_2 & x_1 \\ x_1^* & x_2^* & x_3^* & x_4^* \\ -x_2^* & x_1^* & -x_4^* & x_3^* \\ -x_3^* & x_4^* & x_1^* & -x_2^* \\ -x_4^* & -x_3^* & x_2^* & x_1^* \end{bmatrix} \tag{3.12}$$

- **Complex Orthogonal Design IV**: 3 transmit antennas r=3/4

$$H_C^3 = \begin{bmatrix} x_1 & x_2 & x_3/\sqrt{2} \\ -x_2^* & x_1^* & x_3/\sqrt{2} \\ x_3^*/\sqrt{2} & x_3^*/\sqrt{2} & (-x_1 - x_1 * + x_2 - x_2^*)/2 \\ x_3^*/\sqrt{2} & -x_3^*/\sqrt{2} & (x_2 + x_2^* + x_1 - x_1^*)/2 \end{bmatrix} \tag{3.13}$$

- **Complex Orthogonal Design V**: 4 transmit antennas r=3/4

$$H_C^4 = \begin{bmatrix} x_1 & x_2 & x_3/\sqrt{2} & x_3/\sqrt{2} \\ -x_2^* & x_1^* & x_3/\sqrt{2} & -x_3/\sqrt{2} \\ x_3^*/\sqrt{2} & x_3^*/\sqrt{2} & (-x_1 - x_1 * + x_2 - x_2^*)/2 & (-x_2 - x_2^* + x_1 - x_1^*)/2 \\ x_3^*/\sqrt{2} & -x_3^*/\sqrt{2} & (x_2 + x_2^* + x_1 - x_1^*)/2 & -(x_1 + x_1^* + x_2 - x_2^*)/2 \end{bmatrix} \tag{3.14}$$

3.2 Impact of Channel Estimation Error

There are two reasons of detection errors: low received signal power and receiver noise. In mobile communications, improving either is difficult. This is because the distance that the signal travels can not be limited and the noise figure which depends on the temperature of the environment, can not be easily reduced. Channel estimation is necessary in any coherent communication system or whenever MRC is used. Error in channel estimation will thus cause performance degradation in any coherent system. However, when STBC are used, channel estimation is doubly important. Not only will a correct phase reference not be established,

but orthogonality between Space-Time Code words can not be maintained. Thus channel estimation is an important consideration in STBC

3.2.1 General Case

The received signal at antenna 1 can be expressed as

$$r_1 = x_1 \cdot h_1 + ... + x_n \cdot h_N + n_1, \tag{3.15}$$

where N is the number of transmit antennas, and the desired signal is decision statistic is

$$\hat{s}_i = x_1 \cdot h_1 \cdot \hat{h}_1^* + ... + x_1 \cdot h_N \cdot \hat{h}_N^* + n_1 \cdot \hat{h}_1 + ... + n_N \cdot \hat{h}_N^*. \tag{3.16}$$

If we set $\hat{h} = h + e$ where e is the estimation error, and it is a Gaussian random variable with power inversely related to the channel estimation accuracy $\sigma_e^2 = \frac{1}{SNR_{ch}}$, equation (3.16) becomes

$$\hat{s}_i = x_1 \cdot |h|_1^2 + x_1 \cdot h_1 \cdot e_1 + ... + x_N \cdot |h|_N^2 + x_N \cdot h_N \cdot e_N + n_1 \cdot h_1 + n_1 \cdot e_1 + ... + n_N \cdot h_N + n_N \cdot e_N. \tag{3.17}$$

Now, assuming BPSK model is used, we can represent the probability of bit error as

$$P_e = Prob(Re(s_1 r_1)) < 0 \tag{3.18}$$

As developed in [18], the probability of error P_e can be shown to be equivalent to $Prob\{x^\dagger M x < 0\}$

where

$$x = \begin{bmatrix} h_1 \\ n_1 \\ e_1 \\ \bullet \\ h_N \\ n_N \\ e_N \end{bmatrix} \tag{3.19}$$

is a complex Gaussian vector with correlation matrix R

$$R = \begin{bmatrix} P_1 & 0 & 0 & \bullet & \sqrt{P_1 P_N}\rho_{1N} & 0 & 0 \\ 0 & \sigma_n^2 & 0 & \bullet & 0 & 0 & 0 \\ 0 & 0 & \sigma_e^2 & \bullet & 0 & 0 & 0 \\ \bullet & \bullet & \bullet & \bullet & \bullet & \bullet & \bullet \\ \sqrt{P_1 P_N}\rho_{1N} & 0 & 0 & \bullet & P_N & 0 & 0 \\ 0 & 0 & 0 & \bullet & 0 & \sigma_n^2 & 0 \\ 0 & 0 & 0 & \bullet & 0 & 0 & \sigma_e^2 \end{bmatrix} \tag{3.20}$$

where ρ_{1N} is the correlation between channel channel h_1 and h_N and here we assume equal

power on each transmit antenna. The matrix M is defined as

$$M = \begin{bmatrix} V_{h_1^2} & V_{h_1 n_1} & V_{h_1 e_1} & \bullet & V_{h_N^2} & V_{h_1 n_N} & V_{h_1 e_N} \\ V_{h_1 n_1} & V_{n_1^2} & V_{n_1 e_1} & \bullet & V_{n_1 h_N} & V_{n_1 n_N} & V_{n_1 e_N} \\ V_{h_1 e_1} & V_{n_1 e_1} & V_{e_1^2} & \bullet & V_{e_1 h_N} & V_{e_1 n_N} & V_{e_1 e_N} \\ \bullet & \bullet & \bullet & \bullet & \bullet & \bullet & \bullet \\ V_{h_1 h_N} & V_{h_N^2 n_1} & V_{h_N^2 e_2} & \bullet & V_{h_N^2} & V_{h_N n_N} & V_{h_N e_N} \\ V_{h_1 n_N} & V_{n_N n_1} & V_{n_N e_1} & \bullet & V_{n_N h_N} & V_{n_N^2} & V_{n_N e_N} \\ V_{h_1 e_N} & V_{e_N n_1} & V_{e_N^2} & \bullet & V_{e_N h_N} & V_{e_N n_N} & V_{e_N^2} \end{bmatrix} \tag{3.21}$$

where $V_x y$ is the amplitude of the coefficient associated with the xy term in the decision statistic (3.17). From this, the probability distribution function of $z = x^\dagger M x$ can be determined. To accomplish this, the characteristic function of z is donated as $\Phi_z(s)$:

$$\begin{aligned} \Phi_z(s) &= E\{e^{-sz}\} \\ &= \frac{1}{\pi^3 |R|} \int e^{-s x^\dagger M x} e^{-x R^{-1} x} dx \\ &= \frac{1}{|sM - R^{-1}||R|} \\ &= \frac{1}{|sMR - 1|} \end{aligned} \tag{3.22}$$

The probability distribution function of z is then[18]

$$f(z) = \begin{cases} \sum_{i=1}^{n} -\frac{k_i}{\lambda_i} e^{-\frac{z}{\lambda_i}} & z < 0 \\ \sum_{i=n+p+1}^{N} \frac{k_i}{\lambda_i} e^{-\frac{z}{\lambda_i}} & z > 0 \end{cases} \tag{3.23}$$

where λ_i with $1 \le i \le n$ are the negative eigenvalues of MR, λ_i with $n + p < i \le N$ are the positive eigenvalue of MR, N is the dimension of R and M, and λ_i with $n < i \le n + p$

are the zero eigenvalues. The coefficients k_i are the residues of $\Phi_z(s)$ evaluated at λ_i, and $k_i = \prod_{k \neq i} \frac{\lambda_i}{\lambda_i - \lambda_k}$. The probability of error is then in integration of $f(z)$ from $-\infty$ to 0.

$$\begin{aligned} P_e &= \int_{-\infty}^{0} f(z)dz \\ &= \int_{-\infty}^{0} \sum_{i=1}^{n} -\frac{k_i}{\lambda_i} e^{-\frac{z}{\lambda_i}} dz \\ &= \sum_{i=1}^{n} -\lambda_i (-\frac{k_i}{\lambda_i}) e^{-\frac{z}{\lambda_i \lambda}} |_{-\infty}^{0} \\ &= \sum_{i=1}^{n} k_i \end{aligned} \tag{3.24}$$

3.2.2 Case Study : 8Tx1Rx; 2Tx1Rx and 4Tx1Rx

8Tx1Rx

For analyzing the power of undesired signal distribution, we first built a model for eight transmitter antennas and one receive antenna (see Fig. 3.6).In this model, full rate is desired, so the real orthogonal transmitted signal (G_8) has been employed[3]. The structure of the matrix is shown in equation (3.9) . Assuming the eight channel coefficients are h_1,...,h_8, and

[3]Only the real orthogonal code design can match 8 transmit antennas and one receive antenna

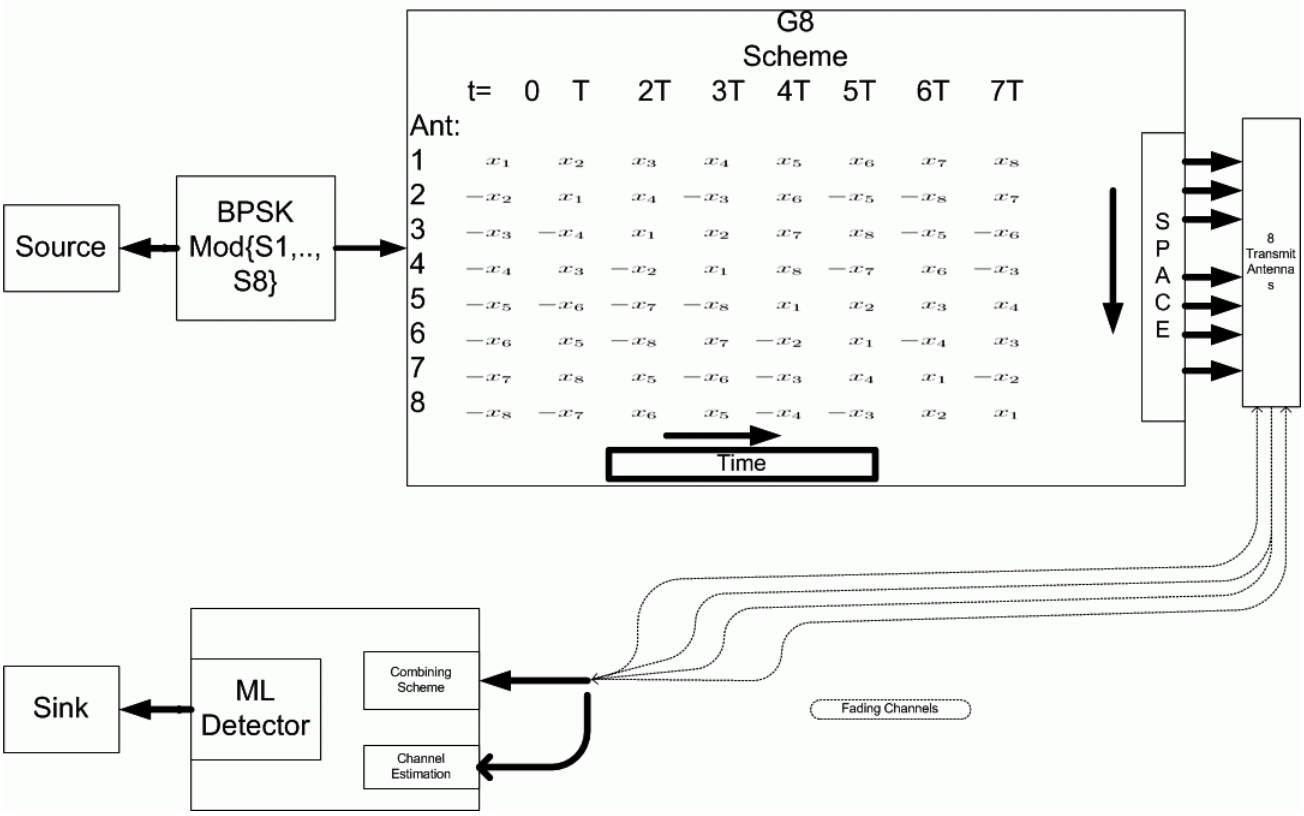

Figure 3.6: 8 Transmit Antennas by 1 receive Antenna Model

the estimated channel coefficients are $\hat{h}_1, ..., \hat{h}_8$, the received signal can be expressed as below

$$\begin{aligned}
r_1 &= x_1h_1 - x_2h_2 - x_3h_3 - x_4h_4 - x_5h_5 - x_6h_6 - x_7h_7 - x_8h_8 + n_1 \\
r_2 &= x_1h_2 + x_2h_1 + x_3h_4 - x_4h_3 + x_5h_6 - x_6h_5 - x_7h_8 + x_8h_7 + n_2 \\
r_3 &= x_1h_3 - x_2h_4 + x_3h_1 + x_4h_2 + x_5h_7 + x_6h_8 - x_7h_5 - x_8h_6 + n_3 \\
r_4 &= x_1h_4 + x_2h_3 - x_3h_2 + x_4h_1 + x_5h_8 - x_6h_7 + x_7h_6 - x_8h_5 + n_4 \\
r_5 &= x_1h_5 + x_2h_6 + x_3h_7 + x_4h_8 - x_5h_1 - x_6h_2 - x_7h_3 - x_8h_4 + n_5 \\
r_6 &= x_1h_6 + x_2h_5 - x_3h_8 + x_4h_7 - x_5h_2 + x_6h_1 - x_7h_4 + x_8h_3 + n_6 \\
r_7 &= x_1h_7 + x_2h_8 + x_3h_5 - x_4h_6 - x_5h_3 + x_6h_4 - x_7h_1 - x_8h_2 + n_7 \\
r_8 &= x_1h_8 - x_2h_7 + x_3h_6 + x_4h_5 - x_5h_4 - x_6h_3 - x_7h_2 + x_8h_1 + n_8 \qquad (3.25)
\end{aligned}$$

The decoder equation can be derived from the eight equations:

$$\begin{aligned}
\hat{x}_1 &= r_1\hat{h}_1^* - r_2\hat{h}_2^* - r_3\hat{h}_3^* - r_4\hat{h}_4^* - r_5\hat{h}_5^* - r_6\hat{h}_6^* - r_7\hat{h}_7^* - r_8\hat{h}_8^* \\
\hat{x}_2 &= -r_1\hat{h}_2^* + r_2\hat{h}_1^* - r_3\hat{h}_4^* + r_4\hat{h}_3^* + r_5\hat{h}_6^* + r_6\hat{h}_5^* + r_7\hat{h}_8^* - r_8\hat{h}_7^* \\
\hat{x}_3 &= -r_1\hat{h}_3^* + r_2\hat{h}_4^* + r_3\hat{h}_1^* - r_4\hat{h}_2^* + r_5\hat{h}_7^* - r_6\hat{h}_8^* + r_7\hat{h}_5^* + r_8\hat{h}_6^* \\
\hat{x}_4 &= -r_1\hat{h}_4^* - r_2\hat{h}_3^* + r_3\hat{h}_2^* + r_4\hat{h}_1^* + r_5\hat{h}_8^* + r_6\hat{h}_7^* - r_7\hat{h}_6^* + r_8\hat{h}_5^* \\
\hat{x}_5 &= -r_1\hat{h}_5^* + r_2\hat{h}_6^* + r_3\hat{h}_7^* + r_4\hat{h}_8^* - r_5\hat{h}_1^* - r_6\hat{h}_2^* - r_7\hat{h}_3^* - r_8\hat{h}_4^* \\
\hat{x}_6 &= -r_1\hat{h}_6^* - r_2\hat{h}_5^* + r_3\hat{h}_8^* - r_4\hat{h}_7^* - r_5\hat{h}_2^* + r_6\hat{h}_1^* + r_7\hat{h}_4^* - r_8\hat{h}_3^* \\
\hat{x}_7 &= -r_1\hat{h}_7^* + r_2\hat{h}_8^* + r_3\hat{h}_5^* - r_4\hat{h}_6^* - r_5\hat{h}_3^* + r_6\hat{h}_4^* - r_7\hat{h}_1^* - r_8\hat{h}_2^* \\
\hat{x}_8 &= -r_1\hat{h}_8^* - r_2\hat{h}_7^* + r_3\hat{h}_6^* + r_4\hat{h}_5^* - r_5\hat{h}_4^* - r_6\hat{h}_3^* - r_7\hat{h}_2^* + r_8\hat{h}_1^*
\end{aligned} \tag{3.26}$$

where $\hat{h}_1 = h_1 + e_1, ..., \hat{h}_8 = h_8 + e_8$. Combining Equation (3.25) and Equation (3.26) results in:

$$\begin{aligned}
\tilde{x}_1 &= x_1|h|_1^2 + x_1h_1e_1 - x_2h_2e_1 - x_3h_3e_1 - x_4h_4e_1 - x_5h_5e_1 - x_6h_6e_1 - x_7h_7e_1 - x_8h_8e_1 + n_1h_1 + n_1e_1 \\
&+ x_1|h|_2^2 + x_1h_2e_2 + x_2h_1e_2 + x_3h_4e_2 - x_4h_3e_2 + x_5h_6e_2 - x_6h_7e_2 - x_7h_8e_2 + x_8h_7e_2 + n_2h_2 + n_2e_2 \\
&+ x_1|h|_3^2 + x_1h_3e_3 - x_2h_4e_3 + x_3h_1e_3 + x_4h_2e_3 + x_5h_7e_3 + x_6h_8e_3 - x_7h_5e_3 + x_8h_6e_3 + n_3h_3 + n_3e_3 \\
&+ x_1|h|_4^2 + x_1h_4e_4 + x_2h_3e_4 - x_3h_2e_4 + x_4h_1e_4 + x_5h_8e_4 - x_6h_7e_4 + x_7h_6e_4 - x_8h_5e_4 + n_4h_4 + n_4e_4 \\
&+ x_1|h|_5^2 + x_1h_5e_5 - x_2h_3e_5 - x_3h_7e_5 - x_4h_8e_5 + x_5h_1e_5 + x_6h_2e_5 + x_7h_3e_5 + x_8h_4e_5 + n_5h_5 + n_5e_5 \\
&+ x_1|h|_6^2 + x_1h_6e_6 + x_2h_5e_6 - x_3h_8e_6 + x_4h_7e_6 - x_5h_2e_6 + x_6h_1e_6 - x_7h_4e_6 + x_8h_3e_6 + n_6h_6 + n_6e_6 \\
&+ x_1|h|_7^2 + x_1h_7e_7 + x_2h_8e_7 + x_3h_5e_7 - x_4h_6e_7 - x_5h_3e_7 + x_6h_4e_7 - x_7h_1e_7 - x_8h_2e_7 + n_7h_7 + n_7e_7 \\
&+ x_1|h|_8^2 + x_1h_8e_8 - x_2h_7e_8 + x_3h_6e_8 + x_4h_5e_8 - x_5h_4e_8 - x_6h_3e_8 + x_7h_2e_8 + x_8h_1e_8 + h_8n_8 + e_8n_8
\end{aligned} \tag{3.27}$$

The transmit signals are normalized, so that the envelope per antenna is equal to $\sqrt{\frac{1}{8}}$, ensuring that the transmit power is equal to the 1 transmit antenna case(ie. we do not increase the transmit signal power), the noise is assumed to be Gaussian and the channel estimation error's power distribution is also Gaussian distributed with $\sigma_e^2 = \frac{1}{SNR_{ch}}$. For analyzing the details, the first row and column analysands are given here. $V_{h_1^2}$=$C_{x_1} * |h|_1^2$, where C_{x_1} is coefficient of x_1, because the envelop of x_1 equals $\sqrt{1/8}$ and the variance of $|h|_1^2$ equals 1, $V_{h_1^2} = \sqrt{1/8} * 1 = \sqrt{1/8}$.

Concerning $V_{h_1 n_1}$ item(note, there is no $\sqrt{8}$ because this item is not related to transmitted signal), since the $|h|_1^2 = 1$ and it is Rayleigh fading, it can be expressed as $1/\sqrt{2} \times (G_a + iG_b)$, here G_a and G_b express Gaussian random number with 0 mean and variance equal 1. Also, the noise is assumed to be complex Gaussian with 0 mean variance 1(the noise level is not considered in here, n_1 = can be expressed as $\sqrt{2} \times (G_c + iG_d)$. As we know, the variance of any Gaussian (with variance 1) times Gaussian (with variance 1 too) $1 \times 1 = 1$, but here the variance of two Gaussian's product is $1/\sqrt{2} \times \sqrt{2}$=$\frac{1}{2}$. Because we only care the real part of the result, $V_{h_1 n_1} = 1/2$.

Concerning $V_{h_1 e_1}$: This item includes 3 components, one is the transmitted signal and its coefficient is $\sqrt{8}$, the product of $h_1 e_2$ is Gaussian and its real part is $\sqrt{2}$, so this item is easily derived as $V_{h_1 e_1}$=$\sqrt{1/8} * 1/2 = \sqrt{1/32}$.

The $V_{h_2 h_1}$, because there is no $h_2 h_1$ term, the value of this item is 0.

Now, let us deal the last special item: $V_{n_1 e_1}$. Because n_1 and e_1 are Gaussian and 0 mean and variance 1, the variance of product's real part is $\sqrt{2} \times \sqrt{2}$=1/2.

$$\mathbf{M}=\begin{bmatrix}
\sqrt{\frac{1}{8}} & \frac{1}{2} & \sqrt{\frac{1}{32}} & 0 & 0 & \sqrt{\frac{1}{32}} & 0 & 0 & \sqrt{\frac{1}{32}} & 0 & 0 & \sqrt{\frac{1}{32}} & 0 & 0 & \sqrt{\frac{1}{32}} & 0 & 0 & \sqrt{\frac{1}{32}} & 0 & 0 & \sqrt{\frac{1}{32}} & 0 & 0 & \sqrt{\frac{1}{32}} \\
\frac{1}{2} & 0 & \frac{1}{2} & 0 & 0 & 0 & 0 & 0 & 0 & 0 & 0 & 0 & 0 & 0 & 0 & 0 & 0 & 0 & 0 & 0 & 0 & 0 & 0 & 0 \\
\sqrt{\frac{1}{32}} & \frac{1}{2} & 0 & \sqrt{\frac{1}{32}} & 0 & 0 & \sqrt{\frac{1}{32}} & 0 & 0 & \sqrt{\frac{1}{32}} & 0 & 0 & \sqrt{\frac{1}{32}} & 0 & 0 & \sqrt{\frac{1}{32}} & 0 & 0 & \sqrt{\frac{1}{32}} & 0 & 0 & \sqrt{\frac{1}{32}} & 0 & 0 \\
0 & 0 & \sqrt{\frac{1}{32}} & \sqrt{\frac{1}{8}} & \frac{1}{2} & \sqrt{\frac{1}{32}} & 0 & 0 & \sqrt{\frac{1}{32}} & 0 & 0 & \sqrt{\frac{1}{32}} & 0 & 0 & \sqrt{\frac{1}{32}} & 0 & 0 & \sqrt{\frac{1}{32}} & 0 & 0 & \sqrt{\frac{1}{32}} & 0 & 0 & \sqrt{\frac{1}{32}} \\
0 & 0 & 0 & \frac{1}{2} & 0 & \frac{1}{2} & 0 & 0 & 0 & 0 & 0 & 0 & 0 & 0 & 0 & 0 & 0 & 0 & 0 & 0 & 0 & 0 & 0 & 0 \\
\sqrt{\frac{1}{32}} & 0 & 0 & \sqrt{\frac{1}{32}} & \frac{1}{2} & 0 & \sqrt{\frac{1}{32}} & 0 & 0 & \sqrt{\frac{1}{32}} & 0 & 0 & \sqrt{\frac{1}{32}} & 0 & 0 & \sqrt{\frac{1}{32}} & 0 & 0 & \sqrt{\frac{1}{32}} & 0 & 0 & \sqrt{\frac{1}{32}} & 0 & 0 \\
0 & 0 & \sqrt{\frac{1}{32}} & 0 & 0 & \sqrt{\frac{1}{32}} & \sqrt{\frac{1}{8}} & \frac{1}{2} & \sqrt{\frac{1}{32}} & 0 & 0 & \sqrt{\frac{1}{32}} & 0 & 0 & \sqrt{\frac{1}{32}} & 0 & 0 & \sqrt{\frac{1}{32}} & 0 & 0 & \sqrt{\frac{1}{32}} & 0 & 0 & \sqrt{\frac{1}{32}} \\
0 & 0 & 0 & 0 & 0 & 0 & \frac{1}{2} & 0 & \frac{1}{2} & 0 & 0 & 0 & 0 & 0 & 0 & 0 & 0 & 0 & 0 & 0 & 0 & 0 & 0 & 0 \\
\sqrt{\frac{1}{32}} & 0 & 0 & \sqrt{\frac{1}{32}} & 0 & 0 & \sqrt{\frac{1}{32}} & \frac{1}{2} & 0 & \sqrt{\frac{1}{32}} & 0 & 0 & \sqrt{\frac{1}{32}} & 0 & 0 & \sqrt{\frac{1}{32}} & 0 & 0 & \sqrt{\frac{1}{32}} & 0 & 0 & \sqrt{\frac{1}{32}} & 0 & 0 \\
0 & 0 & \sqrt{\frac{1}{32}} & 0 & 0 & \sqrt{\frac{1}{32}} & 0 & 0 & \sqrt{\frac{1}{32}} & \sqrt{\frac{1}{8}} & \frac{1}{2} & \sqrt{\frac{1}{32}} & 0 & 0 & \sqrt{\frac{1}{32}} & 0 & 0 & \sqrt{\frac{1}{32}} & 0 & 0 & \sqrt{\frac{1}{32}} & 0 & 0 & \sqrt{\frac{1}{32}} \\
0 & 0 & 0 & 0 & 0 & 0 & 0 & 0 & 0 & \frac{1}{2} & 0 & \frac{1}{2} & 0 & 0 & 0 & 0 & 0 & 0 & 0 & 0 & 0 & 0 & 0 & 0 \\
\sqrt{\frac{1}{32}} & 0 & 0 & \sqrt{\frac{1}{32}} & 0 & 0 & \sqrt{\frac{1}{32}} & 0 & 0 & \sqrt{\frac{1}{32}} & \frac{1}{2} & 0 & \sqrt{\frac{1}{32}} & 0 & 0 & \sqrt{\frac{1}{32}} & 0 & 0 & \sqrt{\frac{1}{32}} & 0 & 0 & \sqrt{\frac{1}{32}} & 0 & 0 \\
0 & 0 & \sqrt{\frac{1}{32}} & 0 & 0 & \sqrt{\frac{1}{32}} & 0 & 0 & \sqrt{\frac{1}{32}} & 0 & 0 & \sqrt{\frac{1}{32}} & \sqrt{\frac{1}{8}} & \frac{1}{2} & \sqrt{\frac{1}{32}} & 0 & 0 & \sqrt{\frac{1}{32}} & 0 & 0 & \sqrt{\frac{1}{32}} & 0 & 0 & \sqrt{\frac{1}{32}} \\
0 & 0 & 0 & 0 & 0 & 0 & 0 & 0 & 0 & 0 & 0 & 0 & \frac{1}{2} & 0 & \frac{1}{2} & 0 & 0 & 0 & 0 & 0 & 0 & 0 & 0 & 0 \\
\sqrt{\frac{1}{32}} & 0 & 0 & \sqrt{\frac{1}{32}} & 0 & 0 & \sqrt{\frac{1}{32}} & 0 & 0 & \sqrt{\frac{1}{32}} & 0 & 0 & \sqrt{\frac{1}{32}} & \frac{1}{2} & 0 & \sqrt{\frac{1}{32}} & 0 & 0 & \sqrt{\frac{1}{32}} & 0 & 0 & \sqrt{\frac{1}{32}} & 0 & 0 \\
0 & 0 & \sqrt{\frac{1}{32}} & 0 & 0 & \sqrt{\frac{1}{32}} & 0 & 0 & \sqrt{\frac{1}{32}} & 0 & 0 & \sqrt{\frac{1}{32}} & 0 & 0 & \sqrt{\frac{1}{32}} & \sqrt{\frac{1}{8}} & \frac{1}{2} & \sqrt{\frac{1}{32}} & 0 & 0 & \sqrt{\frac{1}{32}} & 0 & 0 & \sqrt{\frac{1}{32}} \\
0 & 0 & 0 & 0 & 0 & 0 & 0 & 0 & 0 & 0 & 0 & 0 & 0 & 0 & 0 & \frac{1}{2} & 0 & \frac{1}{2} & 0 & 0 & 0 & 0 & 0 & 0 \\
\sqrt{\frac{1}{32}} & 0 & 0 & \sqrt{\frac{1}{32}} & 0 & 0 & \sqrt{\frac{1}{32}} & 0 & 0 & \sqrt{\frac{1}{32}} & 0 & 0 & \sqrt{\frac{1}{32}} & 0 & 0 & \sqrt{\frac{1}{32}} & \frac{1}{2} & 0 & \sqrt{\frac{1}{32}} & 0 & 0 & \sqrt{\frac{1}{32}} & 0 & 0 \\
0 & 0 & \sqrt{\frac{1}{32}} & 0 & 0 & \sqrt{\frac{1}{32}} & 0 & 0 & \sqrt{\frac{1}{32}} & 0 & 0 & \sqrt{\frac{1}{32}} & 0 & 0 & \sqrt{\frac{1}{32}} & 0 & 0 & \sqrt{\frac{1}{32}} & \sqrt{\frac{1}{8}} & \frac{1}{2} & \sqrt{\frac{1}{32}} & 0 & 0 & \sqrt{\frac{1}{32}} \\
0 & 0 & 0 & 0 & 0 & 0 & 0 & 0 & 0 & 0 & 0 & 0 & 0 & 0 & 0 & 0 & 0 & 0 & \frac{1}{2} & 0 & \frac{1}{2} & 0 & 0 & 0 \\
\sqrt{\frac{1}{32}} & 0 & 0 & \sqrt{\frac{1}{32}} & 0 & 0 & \sqrt{\frac{1}{32}} & 0 & 0 & \sqrt{\frac{1}{32}} & 0 & 0 & \sqrt{\frac{1}{32}} & 0 & 0 & \sqrt{\frac{1}{32}} & 0 & 0 & \sqrt{\frac{1}{32}} & \frac{1}{2} & 0 & \sqrt{\frac{1}{32}} & 0 & 0 \\
0 & 0 & \sqrt{\frac{1}{32}} & 0 & 0 & \sqrt{\frac{1}{32}} & 0 & 0 & \sqrt{\frac{1}{32}} & 0 & 0 & \sqrt{\frac{1}{32}} & 0 & 0 & \sqrt{\frac{1}{32}} & 0 & 0 & \sqrt{\frac{1}{32}} & 0 & 0 & \sqrt{\frac{1}{32}} & \sqrt{\frac{1}{8}} & \frac{1}{2} & \sqrt{\frac{1}{32}} \\
0 & 0 & 0 & 0 & 0 & 0 & 0 & 0 & 0 & 0 & 0 & 0 & 0 & 0 & 0 & 0 & 0 & 0 & 0 & 0 & \frac{1}{2} & 0 & \frac{1}{2} & 0 \\
\sqrt{\frac{1}{32}} & 0 & 0 & \sqrt{\frac{1}{32}} & 0 & 0 & \sqrt{\frac{1}{32}} & 0 & 0 & \sqrt{\frac{1}{32}} & 0 & 0 & \sqrt{\frac{1}{32}} & 0 & 0 & \sqrt{\frac{1}{32}} & 0 & 0 & \sqrt{\frac{1}{32}} & 0 & 0 & \sqrt{\frac{1}{32}} & \frac{1}{2} & 0
\end{bmatrix}$$

Figure 3.7: M-Matrix 8Tx1Rx

The others can be obtained in a similar fashion. Finally we can draw the specific M-matrix for this system. The result is shown in Figure 3.7.

To test this result, simulations were run and compared with the theoretical expression. Monte Carlo simulation is used and the detailed steps are listed below:

- Generate binary data sequence (length is 512 bits);
- Make 7 data sequences based on the original sequence and make them orthogonal with each other, according to the transmission matrix, they are s;

- Generate 8 Rayleigh fading channel and save them for using later, the basic idea is $1/\sqrt{2}(G_a + iG_b)$, G_a, G_b are Gaussian random variables with 0 mean and variance 1, they are h;

- Use the 8 data sequences times the 8 channels. The products are the signal which arrive to each antenna without noise, they are xh;

- Generate 8 same length as any data sequence complex Gaussian random variable and multiplied by the inverse of the SNR desired, they are n;

- Add the noise sequences to each signal arrived on each antenna. The result is $r = xh+n$;

- Generate 8 same length as data sequence complex Gaussian random numbers and multiply channel estimation error level we want to set and add this number to the conjugant of the channel.This step is implemented as $\hat{h} = h^* + e$;

- Use received signal, multiplied by the estimated channel from the previous step and make a decision, if the result is positive, it will be 1, otherwise is -1. Record errors.

- Summing all errors, if the number is less than we set, then go back repeat these steps until the error number is larger or equal to that which we set. In this simulation, the number of error was set at 5000.

After run, the results are obtained and given in Figure 3.8. We can see that there is excellent agreement between the theoretical and simulated results.

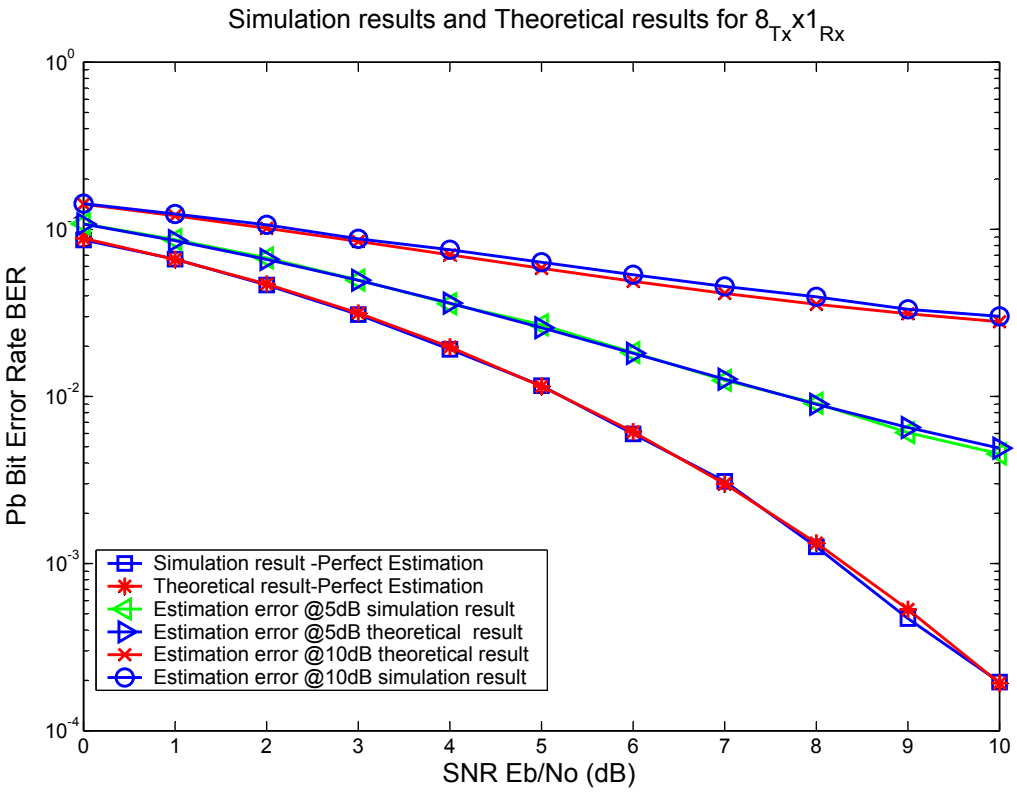

Figure 3.8: Simulation results and theoretical Value for 8Tx1Rx STBC Flat Fading channel

2Tx1Rx and 4Tx1Rx

From Figure 3.3, the 2Tx1Rx's equation can be obtained, they will be:

$$r_0 = x_0 h_0 + x_1 h_1 + n_0$$

$$r_1 = -x_1^* h + x_0^* h_1 + n_1 \tag{3.28}$$

The decision equation for the case of 2Tx1Rx can be obtained as:

$$\hat{x}_0 = \hat{h}_0^* r_0 + \hat{h}_1 r_1^*$$

$$\hat{x}_1 = \hat{h}_1^* r_0 - \hat{h}_0 r_1^* \tag{3.29}$$

$$\mathrm{M}=\begin{bmatrix} \frac{1}{\sqrt{2}} & \frac{1}{2} & \frac{1}{\sqrt{8}} & 0 & 0 & \frac{1}{\sqrt{8}} \\ \frac{1}{2} & 0 & \frac{1}{2} & 0 & 0 & 0 \\ \frac{1}{\sqrt{8}} & \frac{1}{2} & 0 & \frac{1}{\sqrt{8}} & 0 & 0 \\ 0 & 0 & \frac{1}{\sqrt{8}} & \frac{1}{\sqrt{2}} & \frac{1}{2} & \frac{1}{\sqrt{8}} \\ 0 & 0 & 0 & \frac{1}{2} & 0 & \frac{1}{2} \\ \frac{1}{\sqrt{8}} & 0 & 0 & \frac{1}{\sqrt{8}} & 0 & 0 \end{bmatrix}$$

Figure 3.9: M-Matrix 2Tx1Rx

where $\hat{h}_0 = h_0 + e_0$ and $\hat{h}_1 = h_1 + e_1$. Combining Equation (3.28)and Equation (3.29) results in:

$$\hat{x}_0 = x_0|h|_0^2 + x_0 h_0 e_0^* + x_1 h_1 e_0^* + x_0|h|_1^2 + x_0 h_1^* e_1 - x_1 h_0^* e_1 + h_0^* n_0 + h_1 n_1 + n_0 e_0 + n_0 e_1$$

$$\hat{x}_1 = x_0 e_1^* h_0 - x_0 h_1 e_0^* + x_1|h|_1^2 + x_1 h_1 e_1^* + x_1|h|_0^* + x_1 h_0^* e_0^* + h_1^* n_0 - h_0 n_1^* + n_0 e_0^* - n_1^* e_0 \quad (3.30)$$

Following the same rule, the M matrix can be obtained and is shown in Figure 3.9. Following same rules for the 4Tx1Rx case result in Matrix shown in Figure 3.11[18]. The simulation results are shown in Figure 3.10.

Figure 3.12 shows the impact of channel estimation at different values of E_b/N_o. The plots shows the performance versus channel estimation error for different E_b/N_o values: From this plot, we can see that a channel estimation SNR of approximately 15dB will eliminate the impact of channel estimation error. Figure 3.13 plots the results with perfect channel

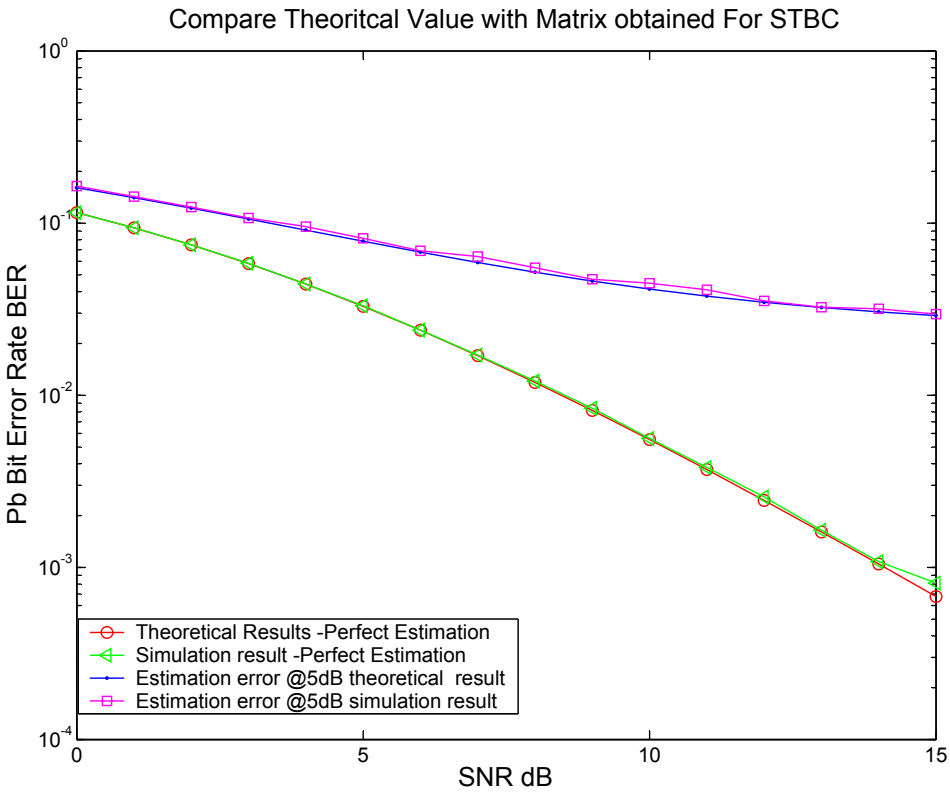

Figure 3.10: Simulation results and theoretical Value for 2Tx1Rx STBC Flat Fading channel estimation along with classical 2/8 branch diversity curves. Again our method agrees with the classic result.

3.2.3 Performance analysis for pilot power

All coherent systems need some method of estimating the phase of the channel. Most of the time this is done using pilot symbols or a pilot channel. However, in most systems only a single transmit antenna is employed with multiple receive antennas. Thus, only a single pilot

$$\mathbf{M}=\begin{bmatrix}
\frac{1}{2} & \frac{1}{2} & \frac{1}{4} & 0 & 0 & \frac{1}{4} & 0 & 0 & 0 & 0 & 0 & 0 \\
\frac{1}{2} & 0 & \frac{1}{2} & 0 & 0 & 0 & 0 & 0 & 0 & 0 & 0 & 0 \\
\frac{1}{4} & \frac{1}{2} & 0 & \frac{1}{4} & 0 & 0 & 0 & 0 & 0 & \frac{1}{4} & 0 & 0 \\
0 & 0 & \frac{1}{4} & \frac{1}{2} & \frac{1}{2} & \frac{1}{4} & 0 & 0 & \frac{1}{4} & 0 & 0 & 0 \\
0 & 0 & 0 & \frac{1}{2} & 0 & \frac{1}{2} & 0 & 0 & 0 & 0 & 0 & 0 \\
\frac{1}{4} & 0 & 0 & \frac{1}{4} & \frac{1}{2} & 0 & \frac{1}{4} & 0 & 0 & 0 & 0 & 0 \\
0 & 0 & 0 & 0 & 0 & \frac{1}{4} & \frac{1}{2} & \frac{1}{2} & \frac{1}{4} & 0 & 0 & \frac{1}{4} \\
0 & 0 & 0 & 0 & 0 & 0 & \frac{1}{2} & 0 & \frac{1}{2} & 0 & 0 & 0 \\
0 & 0 & 0 & \frac{1}{4} & 0 & 0 & \frac{1}{4} & \frac{1}{2} & 0 & \frac{1}{4} & 0 & 0 \\
0 & 0 & \frac{1}{4} & 0 & 0 & 0 & 0 & 0 & \frac{1}{4} & \frac{1}{2} & \frac{1}{4} & \frac{1}{2} \\
0 & 0 & 0 & 0 & 0 & 0 & 0 & 0 & 0 & \frac{1}{2} & 0 & \frac{1}{2} \\
\frac{1}{4} & 0 & 0 & 0 & 0 & 0 & \frac{1}{4} & 0 & 0 & \frac{1}{4} & \frac{1}{2} & 0
\end{bmatrix}$$

Figure 3.11: M-Matrix 4Tx1Rx

channel needs to be transmitted. For STC, however, there are multiple transmit antennas and thus there must be multiple pilot channels to do channel estimation for each transmit antenna. Thus, it seems as though more overhead is required.

When the channel is slowly fading, the noise is the main reason for channel estimation error. The channel estimation error is approximately inversely related to the SNR for traditional wireless communication system with one transmit antenna. However, the channel estimation error is worse than the inverse SNR with STBC if the length of pilot data is fixed. In order to analyze the STBC case (2Tx1Rx is selected), it is necessary to set the power of transmitted data to be P_D (the power of data is transmitted by a single antenna is $P_D/2$) and the noise power to be N. Transmit data consists of two sections: pilot data and information data.

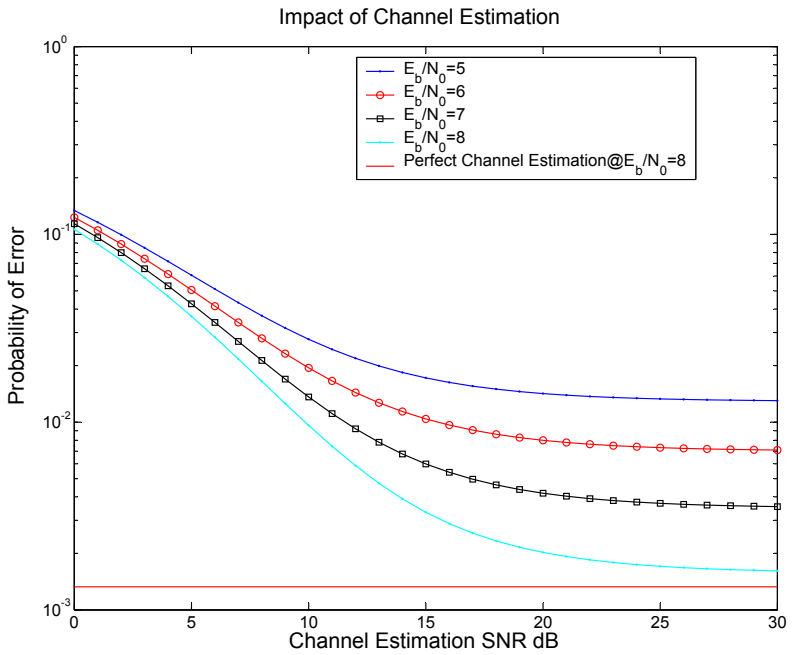

Figure 3.12: Effect of Channel Estimation on 8Tx and 1Rx STBC

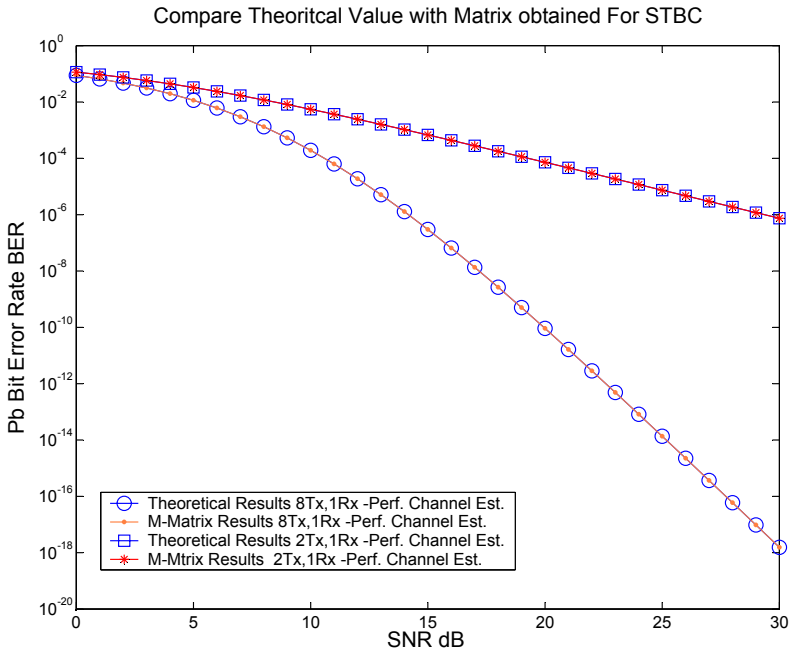

Figure 3.13: Theoretical Results, M-matrix results for 8Tx1Rx, 2Tx1Rx [18]

From the definition of SNR, the channel estimation error is

$$\begin{aligned} SNR_P &= \frac{E_p}{N_0} \\ &= \frac{P_D/2 \times T_P}{N/W} \\ &= \frac{P_D}{2N} = SNR/2 \end{aligned} \tag{3.31}$$

where E_p is power of per pilot bit, W is bandwidth, T_p is pilot's duration (assured to be equal to information in this case), and N is noise power. As we increase the number of transmit antennas, the information data's SNR remains constant, while the pilot data's SNR decreases. So, the only way to keep the channel estimation performance constant is to change the length of the pilot data. Otherwise, the channel estimation error $SNR_P = SNR/8$ for

the 8Tx1Rx STBC system. The BER performance for fixed length pilot data is given below in Figures 3.14 and 3.15. We can see that channel estimation error cripples the performance

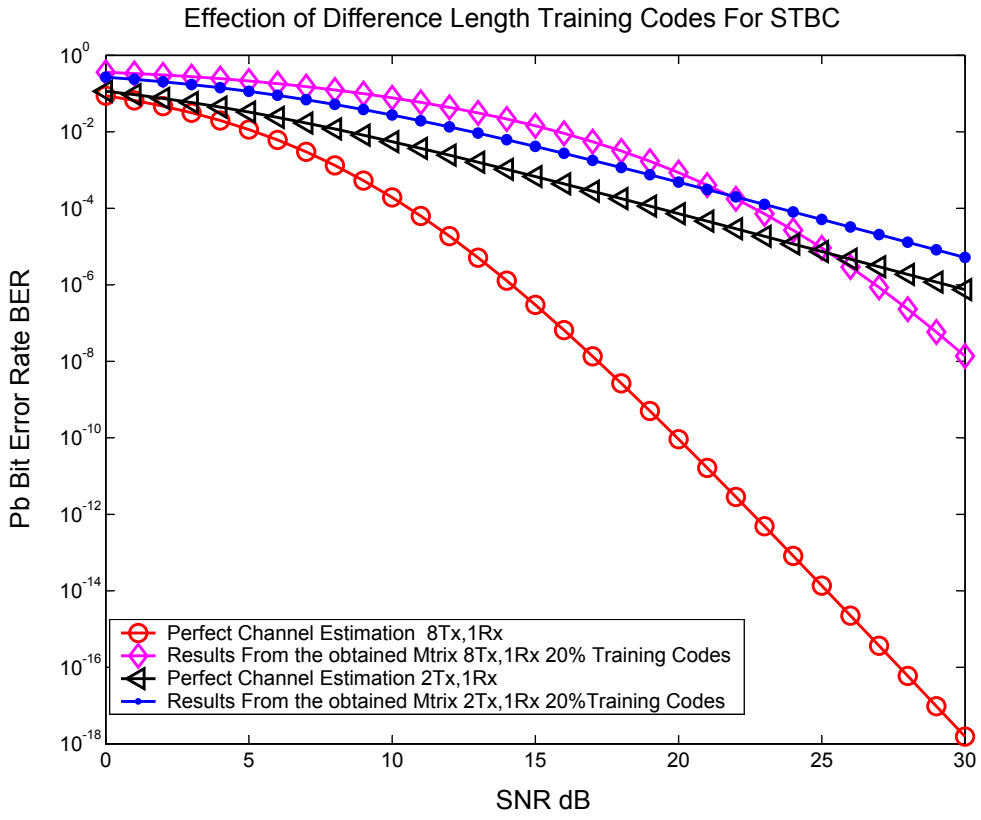

Figure 3.14: Fixed Length Pilot (1/5 Training Code) Data Results

of the 8-antenna scheme, while the performance of the 2-antenna scheme suffers very little. Thus, either we must reduce the throughput of the 8-antenna scheme substantially or use differential encoding techniques.

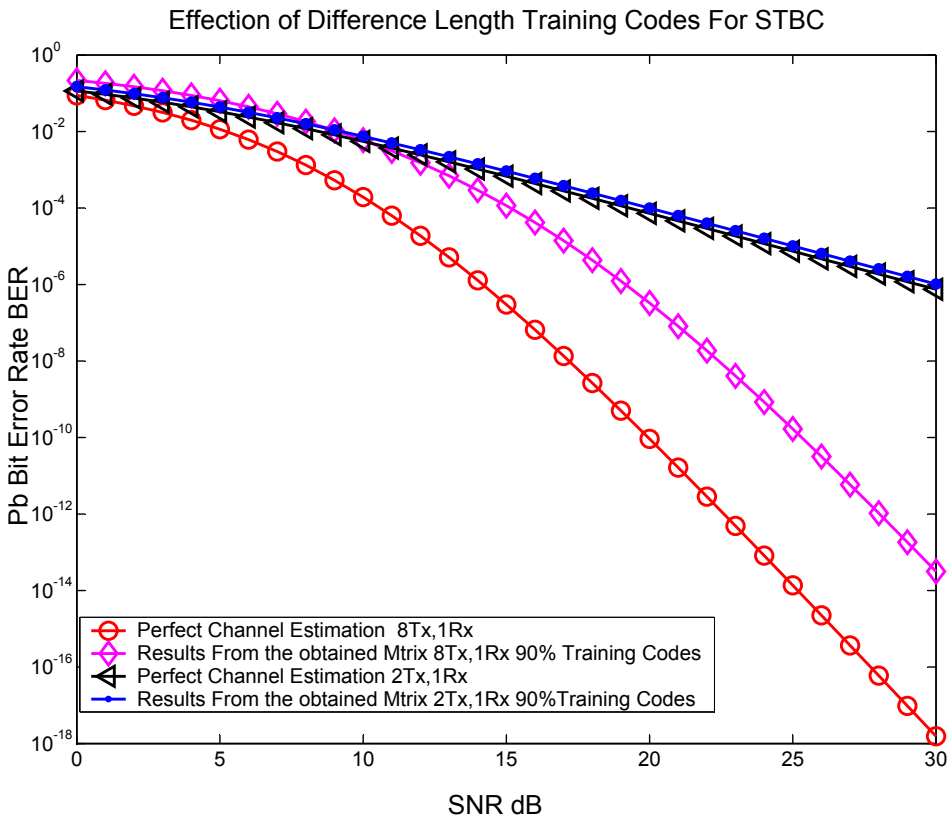

Figure 3.15: Fixed Length Pilot (9/10 Training Code) Data Results

3.3 Frequency Selective Fading

To this point we have made two primary assumptions about the channel: 1) flat fading and 2) the fading from each transmit antenna to any receive antenna are independent. In fact, assumption 1 is invalid for many outdoor situations, because multipath will lead to frequency selective fading resulting in ISI. To overcome it, an equalizer must be used. In this section we investigate the impact of channel estimation error on the frequency selective case.

3.3.1 Frequency selective fading model and Implementation in Simulation

To fully understand frequency selective fading, a channel model will be described. Suppose there are two resolvable paths between one transmit antenna and one receive antenna, the power distribution is [0.5:0.5], and the time difference of arrival is T (one symbol duration). This model is shown in Figure 3.16. The received signal will be

$$r(kT) = s(kT)h1(kT) + s(kT - T)h2(kT - T) + n(KT) \tag{3.32}$$

where k is kth symbol duration, s is transmitted signal, h is channel, and n is noise. For implementing the channel for simulation, a two tap FIR filter is used and its coefficients are $\sqrt{0.5}$ and $\sqrt{0.5}$. The simulation model is shown in Figure 3.17. From Equation (3.32), it can be seen that there is ISI. A discussion was provided in Chapter 1 on how to solve the problem of ISI. The system model is shown in Figure 3.18. Figure 3.19-Figure 3.21 present

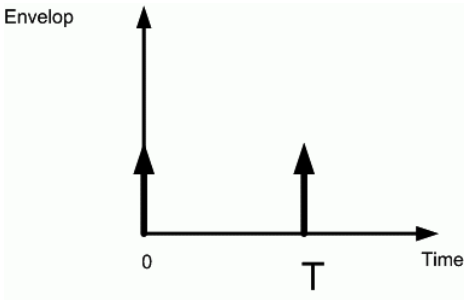

Figure 3.16: Two Ray Equal Power Frequency Selective Model

the performance of two STBC schemes (2Tx2Rx and 8Tx1Rx)in the two ray frequency selective channel. Figure 3.19 shows that a 10dB channel estimation SNR results in 1-3dB

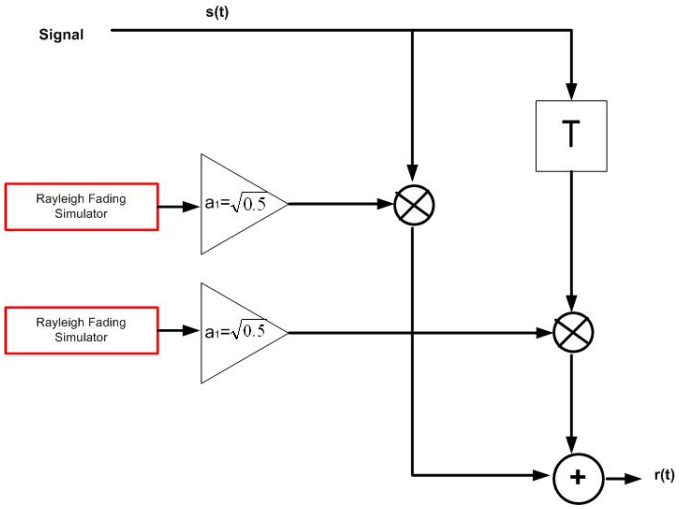

Figure 3.17: Frequency Selective Fading Channel Implementation

degradation, depending on the target BER. In Figure 3.20 and Figure 3.21 we see that the 8Tx/1Rx scheme is more sensitive to channel estimation error, as we expect. Further we see that the frequency selective case does not show greater sensitivity to channel estimation error than the flat fading case.

3.4 Discussion

STBC is a very attractive scheme because of its simplicity especially when complexity is a main issue in system design. However it is not guaranteed to outperform a single antenna scheme when pilot energy is limited (see Figure 3.14). This is because perfect channel estimation is not practical, and channel estimation error can cripple STBC with a large number of transmit antennas. We must either sacrifice data rate (ie. large pilot overhead), use sophisticated channel estimation, or resort to differential encoding/detection. We have

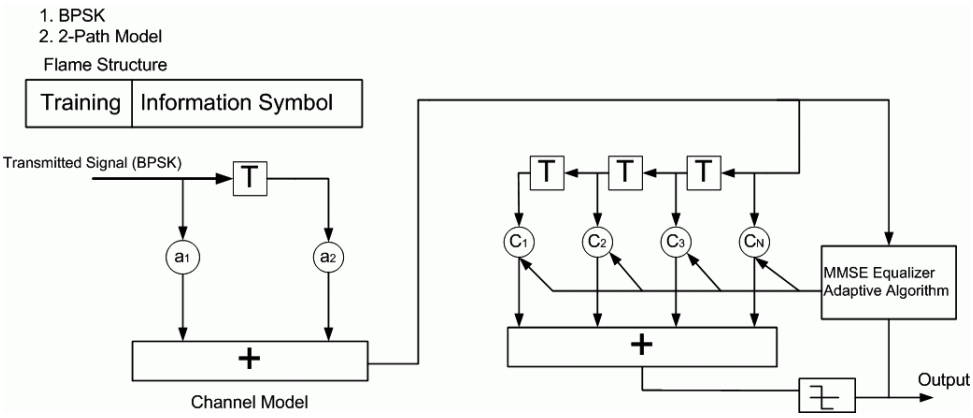

Figure 3.18: STBC's System Model

shown that for STBC with a large number of transmit antennas, channel estimation is a major concern.

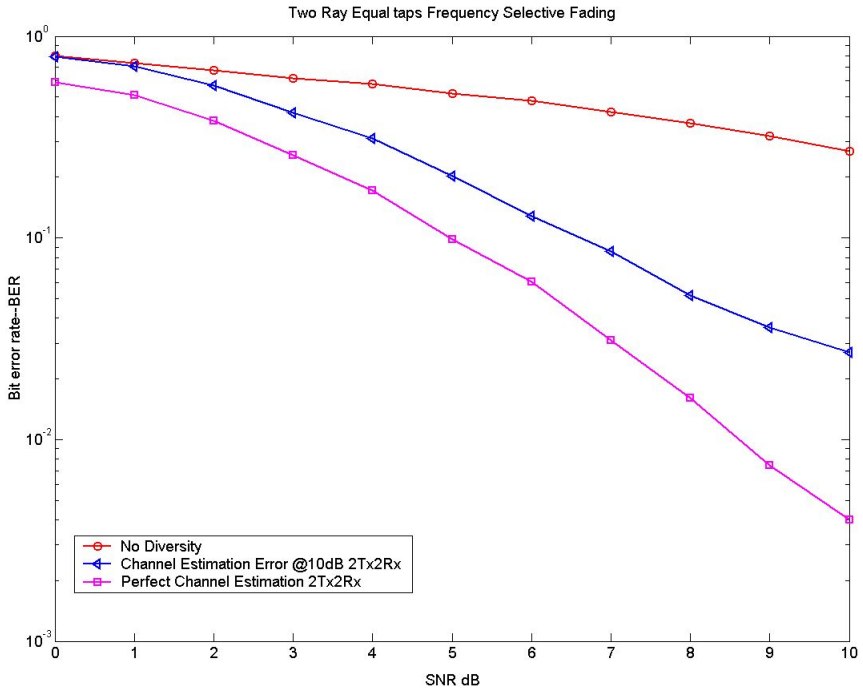

Figure 3.19: Two Tx with Two Rx Two Ray Equal Taps Frequency Selective Fading

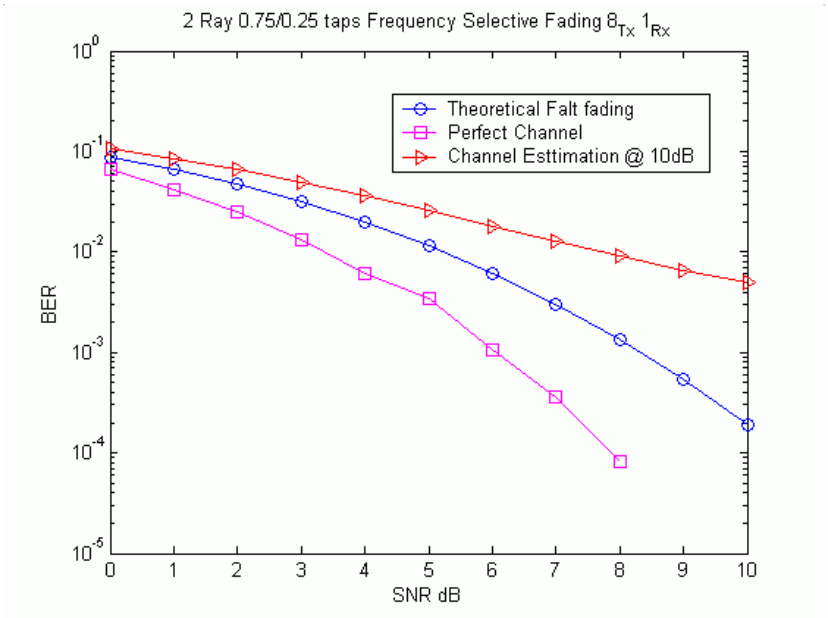

Figure 3.20: Effect of Channel Estimation on Eight Tx with One Rx Two Ray Equal Taps Frequency Selective Fading

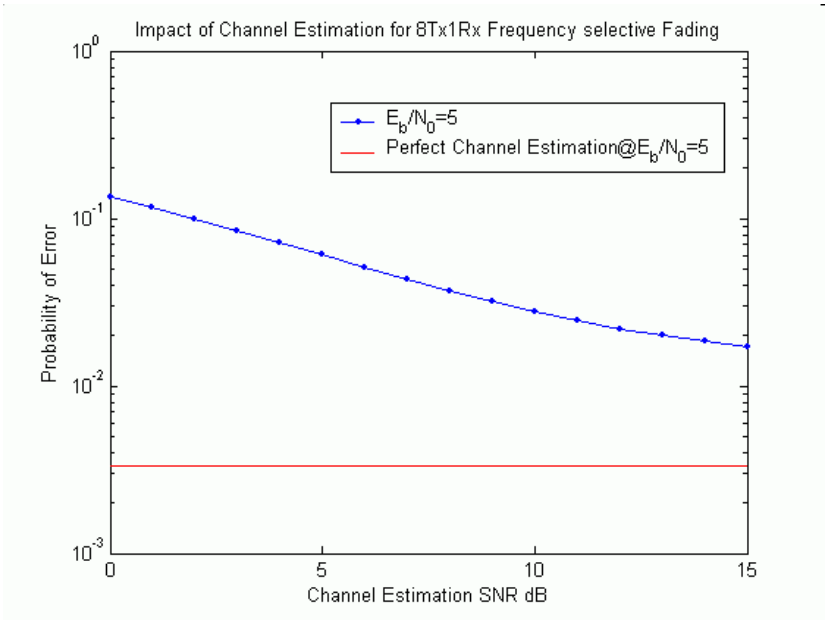

Figure 3.21: Effect of Channel Estimation on 8Tx and 1Rx for two Ray 0.5/0.5 Tap Frequency Selective Fading

Chapter 4

The Impact of Channel Estimation Error on STTC

4.1 Introduction

As discussed in Chapter 2, power and bandwidth are limited resources in a modern communications system and efficient exploitation of these resources will invariably involve an increase in the complexity of the system. It has become apparent over the past few decades that while there are strict limits on the power and bandwidth resources, the complexity of systems could steadily be increased to obtain efficiencies closer to the theoretical limits. Channel coding and interleaving techniques have been recognized as effective techniques for combating the deleterious effects of noise, interference, jamming, fading, and other chan-

nel impairments. Several types of channel codes have been investigated, and they can be roughly classified into two types : block codes, and convolutional codes. Both types provide coding gain to the communication system, but they cost bandwidth or data rate. For solving these issues, Massey [19] proposed that the performance of a coded digital communication system could be improved by treating coding and modulation as a single entity. Ungerboeck later developed the basic principles of trellis-coded modulation (TCM) [20] and identified classes of trellis codes that provide substantial coding gains without increasing bandwidth in AWGN. This property makes TCM very attractive for cellular radio applications where high spectral efficiency is needed due to limited bandwidth resources, and good power efficiency is needed due to limited transmit power.

4.2 Trellis Coded Modulation

TCM schemes combine the operations of coding and modulation and can be viewed as a generalization of convolutional codes. While convolutional codes attempt to maximize the minimum Hamming distance between allowed code symbol sequences, trellis-codes attempt to maximize the minimum Eucliden distance between allowed modulation symbol sequences. TCM experienced an almost immediate and widespread application into high-speed power-efficient and bandwidth-efficient digital modems. In 1984, a variant of the Ungerboeck 8-state 2-D trellis code was adopted by CCITT for both 14.4kb/s leased-line modems and the 9.6kb/s switched-network modems [21].

4.2.1 TCM Encoding

Conventional convolutional codes realize a coding gain at the expense of data rate or bandwidth. Although such coding schemes are attractive for power-limited applications, they are not suitable for bandwidth-limited applications [3]. Underboeck showed that a coding gain can be achieved without sacrificing data rate or bandwidth by using a rate-$m/(m+r)$ convolutional encoder, and mapping the code bits onto signal points x_k through a technique called "mapping by set partitioning" [20]. This combination of coding and modulation is termed "Trellis coded modulation (TCM)", and has these basic features:

- An expanded signal constellation is used that is larger than the one necessary for uncoded modulation at the same data rate;
- The expanded signal constellation is partitioned such that the intra-subset minimum squared Euclidean distance is maximized at each step in the partition chain; and
- Convolutional encoding and signal mapping are used so that only certain sequences of signal points are allowed.

The critical step in the design of Ungerboeck's codes is the method of mapping the outputs of the convolutional encoder to points in the expanded signal constellation.

The trellis encoder model of 4-state 8-PSK is shown in Figure 4.1.

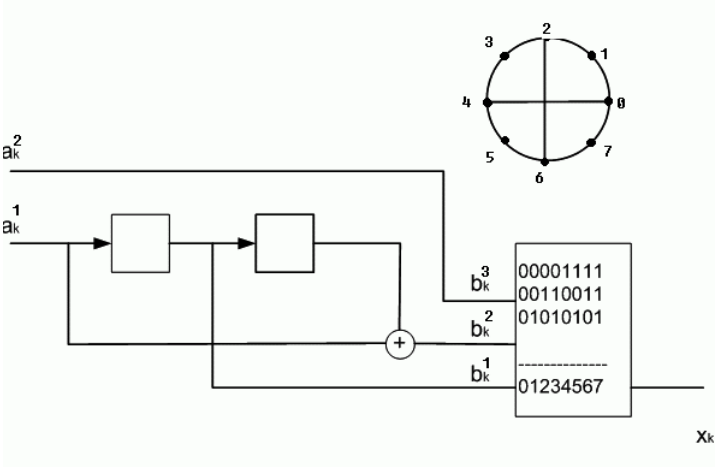

Figure 4.1: Encoder and signal mapping for the 4-state 8-PSK Ungerboeck trellis code

4.2.2 TCM decoding

The task of a convolutional decoder is to estimate the maximum likelihood path that the message has traversed through the encoding trellis. If all input message sequences are equal, a decoder that will achieve the minimum probability of error is one that compares the conditional probabilities $P(\mathbf{Z}|\mathbf{U}^{(m)})$ where $\mathbf{Z}$ is received sequence of waveforms, and $\mathbf{U}^{(m)}$ is one of the possible transmitted sequences of waveforms, and chooses the maximum. This decision-making criterion, is known as the maximum likelihood (ML) criteria. Since an ML decoder will choose the trellis path whose corresponding sequence $\mathbf{U}^{(m)}$ is at the minimum distance to the received sequence $\mathbf{Z}$, the ML problem is identical to the problem of finding the shortest distance through the trellis diagram.

Because a convolutional code is a linear code, the set of distances that must be examined is independent of which sequence is selected as a test sequence. Therefore, there is no loss in generality in selecting an all-zeros sequence, which is shown as a dashed line in Figure

4.2. Assuming that the all-zeros sequence is transmitted, an error event is identified as a divergence from the all-zero path followed by a remerging with the all-zeros path.

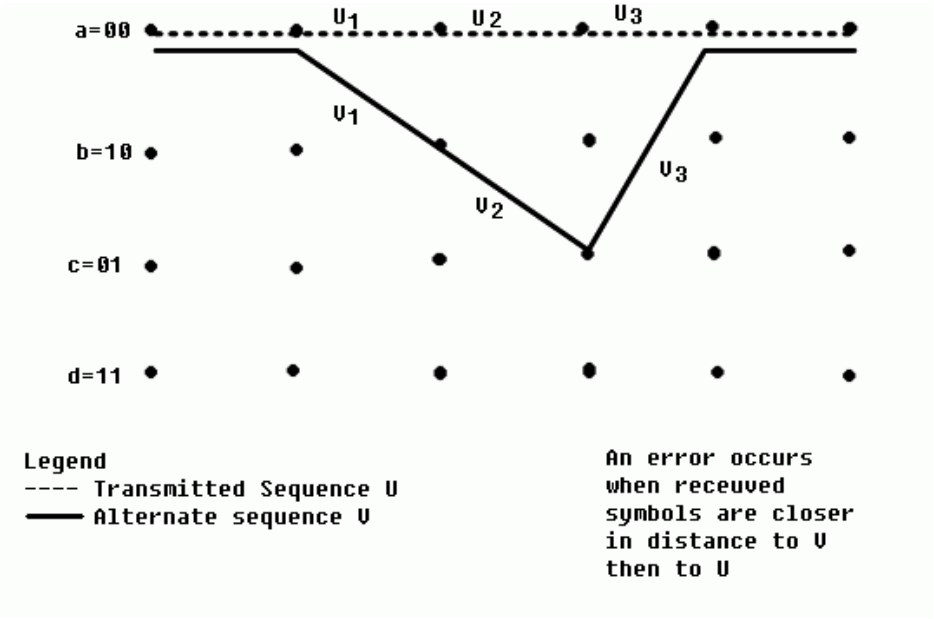

Figure 4.2: Illustration of an error events

Coding Gain

Using soft-decision, ML decoding, and assuming unit average signal power and Gaussian noise with variance σ^2 per dimension, a lower bound on the error-event probability can be expressed in terms of the free distance [22][23] as

$$P_e \geq Q\left(\frac{d_f}{2\sigma}\right) \tag{4.1}$$

where $Q(\bullet)$ is Q function. Note, here "error event" is used rather than "bit-error", because the error might entail more than one flawed bit. At high SNR, the bound in Equation (4.1)

is asymptotically exact. Taking the asymptotic coding gain G compared with some uncoded reference system with the same average signal power and noise variance, the coding gain can be derived as

$$G(dB) = \left(\frac{E_b}{N_0}\right)_u - \left(\frac{E_b}{N_0}\right)_c \qquad (dB)^1 \tag{4.2}$$

This equation, in effect, summarizes the primary goal of TCM code construction, to achieve a free distance that exceeds the minimum distance between uncoded modulation signals (at the same information rate, bandwidth, and power).

4.3 Space-Time Trellis Codes

Space-time trellis coding takes advantage of the coding gain provided by trellis codes and the advantage of diversity provided by STC. The main disadvantage is that they are difficult to design at both the encoder and decoder.

There are two parts in the trellis encoder: one is the convolutional encoder, and the second part is the mapping function. The mapping function follows the convolutional encoding. The structure is shown in Figure 4.3. The function of the mapper is to generate the trellis $x^i = \tau(b^i, s^i)$,where τ is mapper function, b^i is input bit, s^i is state of FSM (Finite-State Machine) and x^i is output of mapper function. The distance of two branches is $d^2 = \|x^1 - x^2\|^2$, and it relates to the branch label. From Figure 4.4, we can easily obtain the distance.

[1] $(E_b/N_0)_u$ and $(E_b/N_0)_c$ represent the required E_b/N_0 for the uncoded system and the coded system to achieve a specific bit error rate, respectively.

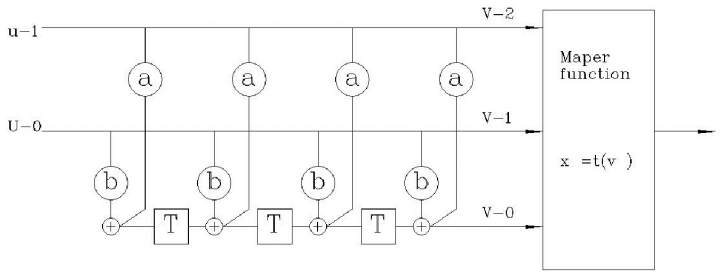

Figure 4.3: General structure of a trellis encoder

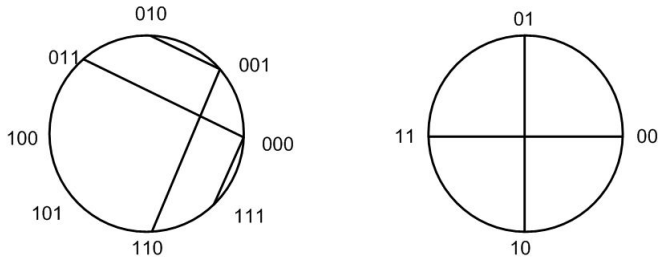

Figure 4.4: 8PSK and QPSK signal sets

4.3.1 Code Construction

According to [24] the system model is as follows. We assume a MIMO system with N transmit and M receive antennas. The channel is comprised of $N \times M$ slowly varying channels, where each channel is assumed to obey narrowband Rayleigh fading.

Then, the following code vector is transmitted simultancously from N transmit antennas at time instant l:$\mathbf{c} = [c_1(l), ...c_N(l)]^T$. The MIMO channel matrix $\mathbf{H}$ is given as:

$$\mathbf{H} = \begin{bmatrix} a_{1,1} & a_{1,2} & \cdots & a_{1,N} \\ a_{2,1} & a_{2,2} & \cdots & a_{2,N} \\ \vdots & \vdots & \ddots & \vdots \\ a_{M,1} & a_{M,1} & \cdots & a_{M,N} \end{bmatrix} \tag{4.3}$$

Finally, the received signal vector can be expressed as: $\mathbf{r}(l) = \mathbf{H} \cdot \mathbf{c}_l + \mathbf{n}(l)$. If the ML receiver is used, the probability that the receiver decides erroneously in favour of a signal, $\mathbf{e} = e_1^1 e_2^2 \cdots e_1^n e_2^1 e_2^2 \cdots e_2^n \cdots e_l^n$, assuming that $\mathbf{c} = c_1^1 c_1^2 \cdots c_1^n c_2^1 c_2^2 \cdots c_2^n \cdots c_l^1 c_l^2 \cdots c_l^n$ was transmitted and idea' channel state information (CSI) is available can be upper bounded as [24]

$$P(\mathbf{c} \rightarrow \mathbf{e}|\mathbf{H}) \leq e^{-d^2(\mathbf{c},\mathbf{e})} \tag{4.4}$$

where

$$d^2(\mathbf{c}, \mathbf{e}) = \frac{E_s}{4N_0} \sum_{j=1}^{M} \mathbf{h}_j \cdot \mathbf{A(c,e)} \cdot \mathbf{h}_j^* \tag{4.5}$$

where $\mathbf{A(c,e)} = \mathbf{B(c,e)} \cdot \mathbf{B}^*\mathbf{(c,e)}$. The matrix $\mathbf{A}$ is called the distance matrix and the matrix $\mathbf{B}$ is the difference error matrix which is compromised of the transmitted code vector sequence $\mathbf{c}$ and the decoded erroneous code vector $\mathbf{e}$.

If $r \leq min(N, M)$ is the rank of $\mathbf{A}$ and $\lambda_1, \lambda_2, \cdots \lambda_r$ are its non-zero eigenvalues, then a final expression for the error probability for $\mathbf{r} \cdot M \leq 3$ can be given as[24]:

$$P(\mathbf{c} \rightarrow \mathbf{e}|\mathbf{H}) \leq \left(\prod_{i=1}^{r} \lambda_i \right) \cdot \left(\frac{1}{4} \frac{E_s}{N_0} \right)^{-r \cdot M} \tag{4.6}$$

where the first product term represents coding gain and the second term diversity gain. Accordingly, the design criteria for STTCs for $r \cdot M \leq 3$ are specified such as to maximize coding gain by maximising the determinant of the distance matrix $\mathbf{A}$.

A similar expression for the error probability for $r \cdot M \leq 3$ is derived by [25] as:

$$P(\mathbf{c} \rightarrow \mathbf{e}|\mathbf{H}) \leq \frac{1}{2} exp \left(-M \frac{E_s}{4N_0} \sum_{i=1}^{N} \lambda_i \right) \tag{4.7}$$

Therefore, the coding gain is maximised by maximising the trace of the distance matrix $\mathbf{A}$.

4.3.2 Code Design

A two-branch feedforward shift register with memory order v is used to model a 4-PSK STTC encoder with n_T transmit antennas. At time t, two binary inputs, I_t^1 and I_t^2, are feed into the first and the second branches with memory order v_1 and v_2, respectively, where I_t^1 is the most significant bit. $v = \sum_{i=1}^{2} v_i$ and $v_i = \lfloor (v + i - l)/2 \rfloor$, where $\lfloor x \rfloor$ denotes the maximum integer not larger than x. The two streams of input bits are passed through their respective shift register branches and multiplied by coefficient vectors **a** and **b**. The symbol transmitted on the kth antenna at time t is computed as

$$x_t^k = \sum_{p=0}^{v_1} I_{t-p}^1 a_p^k + \sum_{q=0}^{v_2} I_{t-q}^2 b_q^k \qquad mod4 \qquad k = 1, 2 \tag{4.8}$$

where a_p and b_q are arranged in an alternate order to form the generator matrix [26].

4.3.3 STTC Generator Matrix

From Equation (4.8), we can obtain the generator matrix. The detailed steps are listed in [15]. There are three kinds of main generator matrices. If we define the generator matrix as

$$G = \begin{bmatrix} a_0^1 & b_0^1 & a_1^1 & b_1^1 & ... & b_n^1 & b_{n+1}^1 \\ a_0^2 & b_0^2 & a_1^2 & b_1^2 & ... & b_n^2 & b_{n+1}^2 \end{bmatrix} \tag{4.9}$$

there are several different results from Taroky, Baro and Z. Chen[25]. They are shown in Tables 4.2 and 4.3.

The matrices for 8-PSK are given in the papers, so here we will not list them. Please

States	a_0^1, a_0^2	a_1^1, a_1^2	a_2^1, a_2^2	a_3^1, a_3^2	b_0^1, b_0^2	b_1^1, b_1^2	b_2^1, b_2^2	b_3^1, b_3^2
4	(0,2)	(2,0)	–	–	(0,1)	(1,0)	–	–
8	(0,2)	(2,0)	–	–	(0,1)	(1,0)	(2,2)	–
16	(0,2)	(2,0)	(0,2)	–	(0,1)	(1,2)	(2,0)	–
32	(0,2)	(2,2)	(3,3)	–	(0,1)	(1,1)	(2,0)	(2,2)

Table 4.1: 4-PSK trellis codes for 2Tx by Tarokh[11]

States	a_0^1, a_0^2	a_1^1, a_1^2	a_2^1, a_2^2	a_3^1, a_3^2	b_0^1, b_0^2	b_1^1, b_1^2	b_2^1, b_2^2	b_3^1, b_3^2
4	(2,2)	(1,0)	–	–	(0,2)	(3,1)	–	–
8	(2,2)	(2,0)	–	–	(0,1)	(1,0)	(2,2)	–
16	(0,2)	(2,0)	(0,2)	–	(2,1)	(1,2)	(2,0)	–
32	(0,2)	(2,3)	(1,2)	–	(2,2)	(1,2)	(2,3)	(2,0)

Table 4.2: 4-PSK trellis codes for 2Tx from Baro [26]

States	a_0^1, a_0^2	a_1^1, a_1^2	a_2^1, a_2^2	a_3^1, a_3^2	b_0^1, b_0^2	b_1^1, b_1^2	b_2^1, b_2^2	b_3^1, b_3^2
4	(0,2)	(1,2)	–	–	(2,3)	(2,0)	–	–
8	(2,2)	(2,1)	–	–	(2,0)	(1,2)	(0,2)	–
16	(1,2)	(1,3)	(3,2)	–	(2,0)	(2,2)	(2,0)	–
32	(0,2)	(3,1)	(3,3)	(3,2)	(2,2)	(2,2)	(0,0)	(2,0)

Table 4.3: 4-PSK trellis codes 2Tx from Z. Chen.[25]

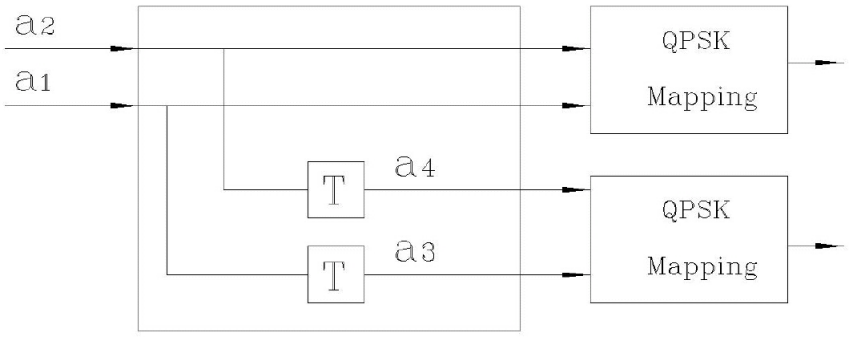

Figure 4.5: 8PSK and QPSK signal sets

see references [11],[26] and [25] if interested. Once the generator matrix is obtained, the implementation of the encoder, shown in Figure 4.5 is straightforward. [2]

4.3.4 STTC Transmitter and Receiver models

The original STTC's system designer is Vahid Tarokh. In 1998 [11], he presented a general architecture for a narrowband TDMA/STCM-based modem with N transmit antennas suitable for wireless communications. Tarokh's block model is shown in Figure 4.6 [11]. The information bits are encoded by an ST channel encoder and the output of the ST encoder is split into two streams of the encoded modulation system. Each stream of encoded symbols is then independently interleaved using a block symbol-by-symbol interleaver. A pilot sequence is attached to symbols after interleaving. The last section is pulse shaper. Typically raised

[2]This figure is for a 4 state encoder

cosine pulse (RC) shaping is used. The $p(t)$ of RC is given by [3]

$$p(t) = \frac{4\epsilon}{\pi\sqrt{T_s}} \cdot \frac{cos((1+\epsilon)\pi t/T_s) + \frac{sin((1-\epsilon)\pi t/T_s)}{(4\epsilon/T_s)}}{(4\epsilon/T_s)^2 - 1} \tag{4.10}$$

where ϵ is the bandwidth expansion or roll-off factor. Tarokh truncated $p(t)$ to $\pm 3T_s$ around $t = 0$. The signal after the pulse shaper can be written as:

$$s_i(t) = \sqrt{E_s} \cdot \sum_l c_i(l) p(t - lT_s) \quad i = 1, 2. \tag{4.11}$$

.

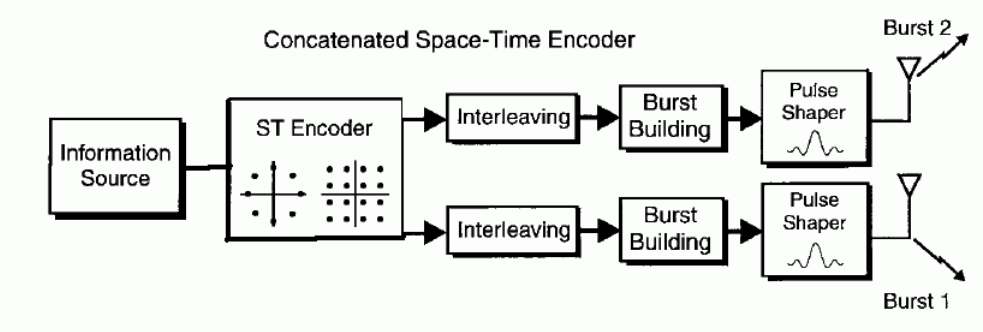

Figure 4.6: Base station transmitter with STTC and two antennas [11]

Figure 4.7 shows the receiver design. Any receiver design must be symmetrical to the transmitter; the first section of the receiver is the matcher filter and its impulse response is $\bar{p}(t)$, which is matched to the transmit pulse shape $p(t)$ given in Equation 4.10. The second part of the receiver is deinterleaving; it deinterleaves the signal after the matched filter. The last part is a vector maximum likehood sequence decoder.

Here, a 4-state 4PSK 2Tx case is discussed. If the trellis diagram of the S/T code is

$$S_i{=}X_0Y_0 \quad X_1Y_1 \quad X_2Y_2 \quad X_3Y_3$$

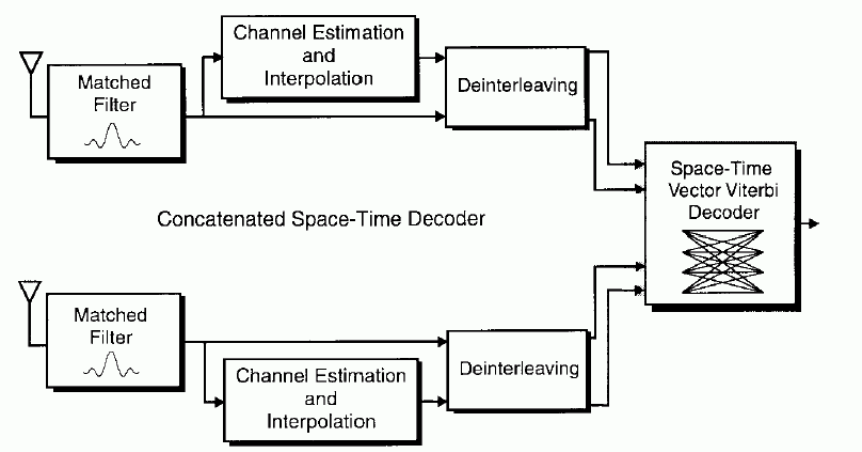

Figure 4.7: Mobile receiver with STTC and two receiver antennas [11]

the current state is S_i, the input symbol is "j", Antenna ♯1 transmits X_j and Antenna ♯2 transmits Y_j, and the next state is S_j. An example is shown in Figure 4.8.

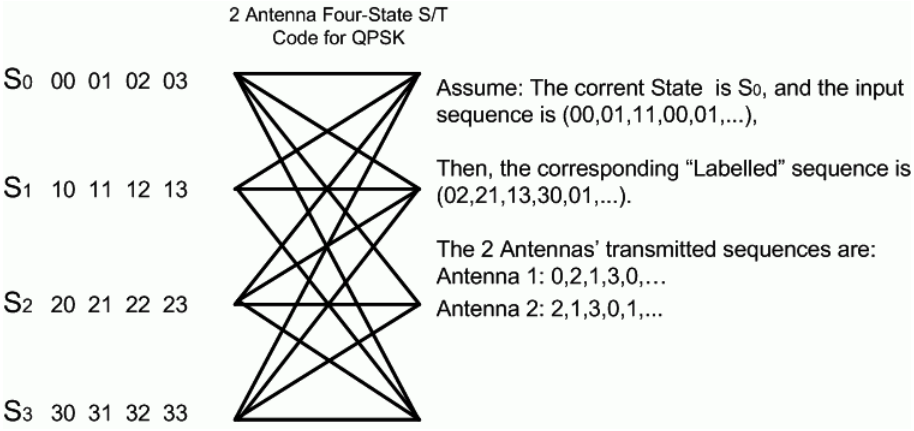

Figure 4.8: Example of 2 Tx 4-state Trellis encoder

From the receiver model, we can see the channel estimation is an important section. We will initially assume that channel estimation is perfect. For analyzing the impact of channel estimation, we will add Gaussian noise to the perfect channel estimation.

4.4 STTC performance

The performance of STTC is unlike STBC, which allows calculation of the exact error performance. From theoretical analysis, we can only derive an upper bound for STTC performance. All the simulation results should be better than the bound. Ran Gozali has provided a very good way to analyze STTC in his dissertation [15]. Here, only an outline of his results are given.

The process of analysis can be separated into six steps. They are:

- Form the modified state diagram of the code;
- Evaluate the matrix A per trellis branch;
- Compute the corresponding eigenvalues $\lambda(A)$;
- Label the modified state diagram with the averaged branch labels;
- Write the state equation to compute $\overline{T(D, L, I)}$;
- Evaluate an upper bound for the code.

Using these rules, the analysis steps are shown below:

1) The branch label of the state modified diagram is described by

$$a(D, I) = I^{n_d} D^{d^2(c_t, e_t|\alpha_{i,j})} \tag{4.12}$$

where c_t corresponds to the transmitted set at time t of n_T all-zero symbols, e_t corresponds to the erroneously decided set of n_T coded symbols, n_d is the Hamming distance

and $d^2(c_t, e_t|\alpha_{i,j})$ is the conditional squared Euclidean distance between the two sets.

2) The matrix A of (p, q) trellis branch is

$$A_{pq} = (c_t^p - e_t^p)\overline{c_t^q - e_t^q} \tag{4.13}$$

.

3) The eigenvalues of A can be easily to computed from Equation 4.13.

4) Equation (4.12) can be rewritten as

$$a(D, I) = I^{n_d} D^{\sum_{j=1}^{n_r} \sum_{i=1}^{n_T} \lambda_i |\beta_{i,j}|^2} \tag{4.14}$$

If we average Equation (4.14) with respect to the Rayleigh pdf, we obtain:

$$\overline{a(D, I)} = I^{n_d} \prod_{i=1}^{n_t} (1 + \gamma\lambda_i)^{-n_r} \tag{4.15}$$

5) Equation (4.15) is incorporated into the modified state diagram, so that the average transfer function of the code is derived and it is denoted $\overline{T(D, L, I)}$.

6) This average transfer function is then differentiated with respect to I to obtain the desired bit-error probability upper bound

$$P_b < \frac{1}{2n} \frac{\overline{\partial T(D, L, I)}}{\partial I}|_{I=1, D=e^{-E_s/4N_0}} \tag{4.16}$$

Here the simulation result to upper bound drawing is shown in Figure 4.4.

4.5 Simulation results

Simulation results are given in Figure 4.9 - Figure 4.11 for flat fading. Figure 4.10 is based on [26], and Figure 4.11 is based on [25]. From the two figures, we can see that the code

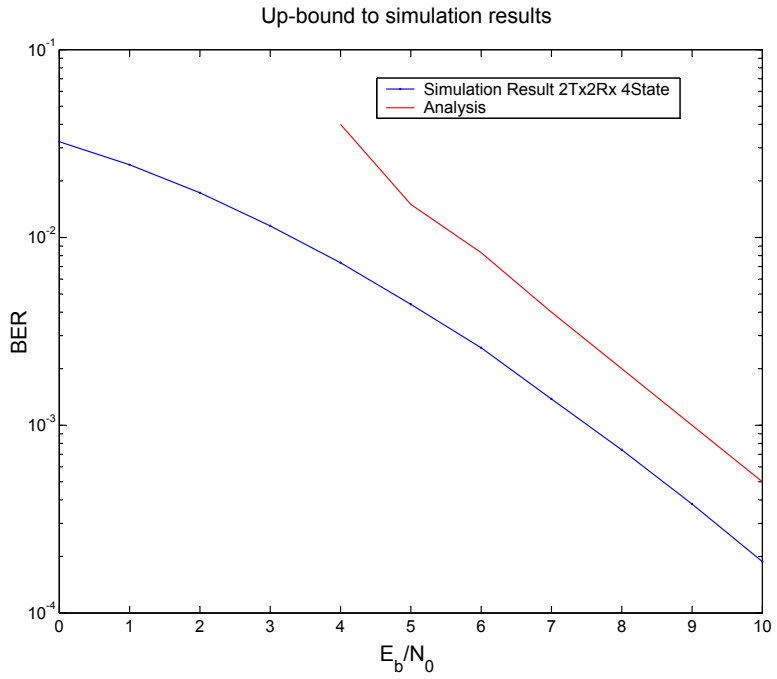

Figure 4.9: Error Bounds for 4 State STTC over Flat Rayleigh Fading Channel

from [25] provides better performance than [26]. All the results are over the slow nonselective channel. We see that, unlike STBC, channel estimation error has little impact.

Figure 4.12 presents simulation results which show the impact of channel estimation error at a channel SNR of 10dB. STBC's results are also included. From the comparison, we can find that STTC's performance is better than STBC's, and STBC is more sensitive to channel estimation error. Comparing Figure 4.13 with Figure 3.9, we see STTC is much more robust to channel estimation error. The reason why the STTC is relatively insensitive to channel error is that the decoder uses the Viterbi algorithm. This algorithm uses the received bits for reference bits. The channel estimation error does impact data decisions, but the decision

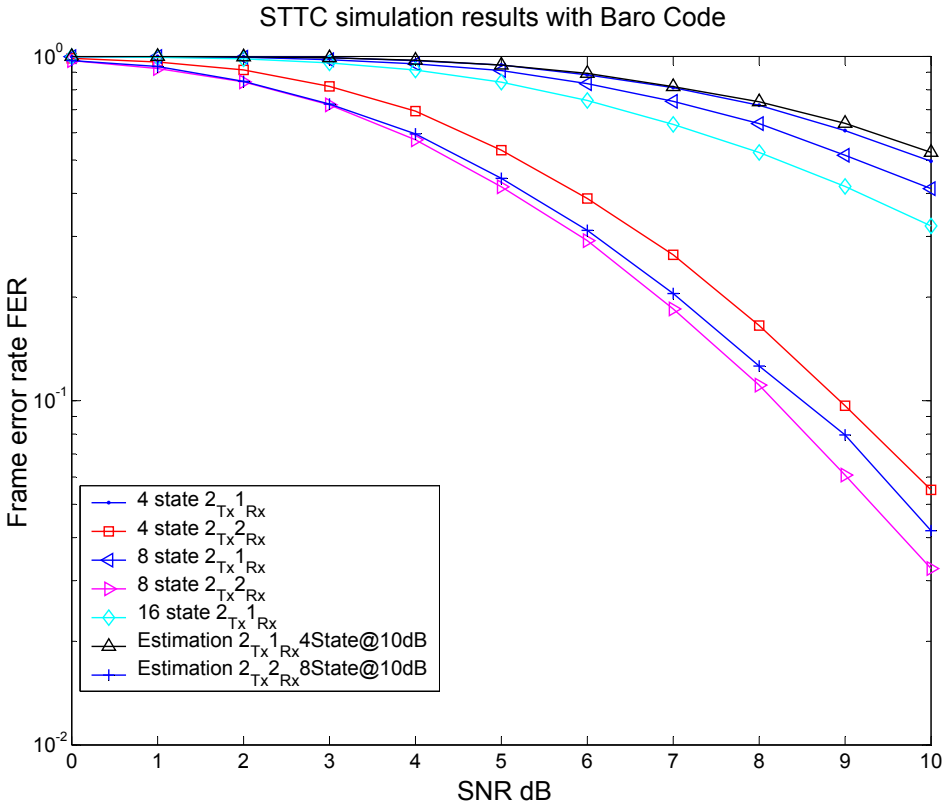

Figure 4.10: Simulation Results for STTC Using Code of [26]

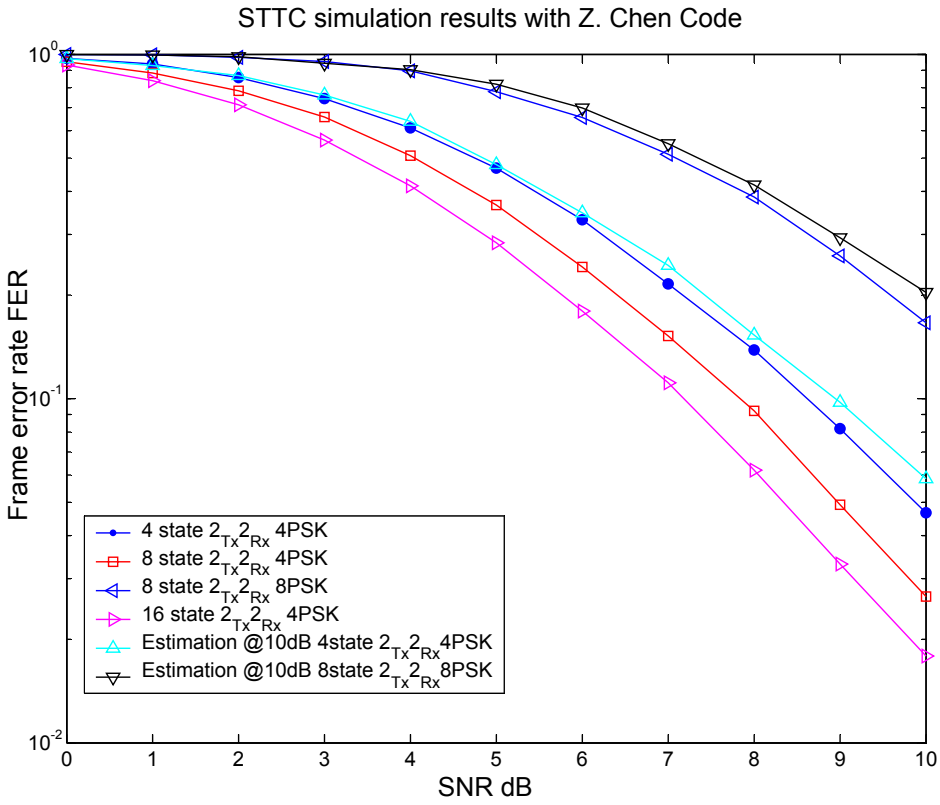

Figure 4.11: Simulation Results for STTC Using Code of [25]

rule does not depend on the pre-decision data, it depends the path distance. If channel estimation errors does not result in changing the distance between code words, there is no impact on performance.

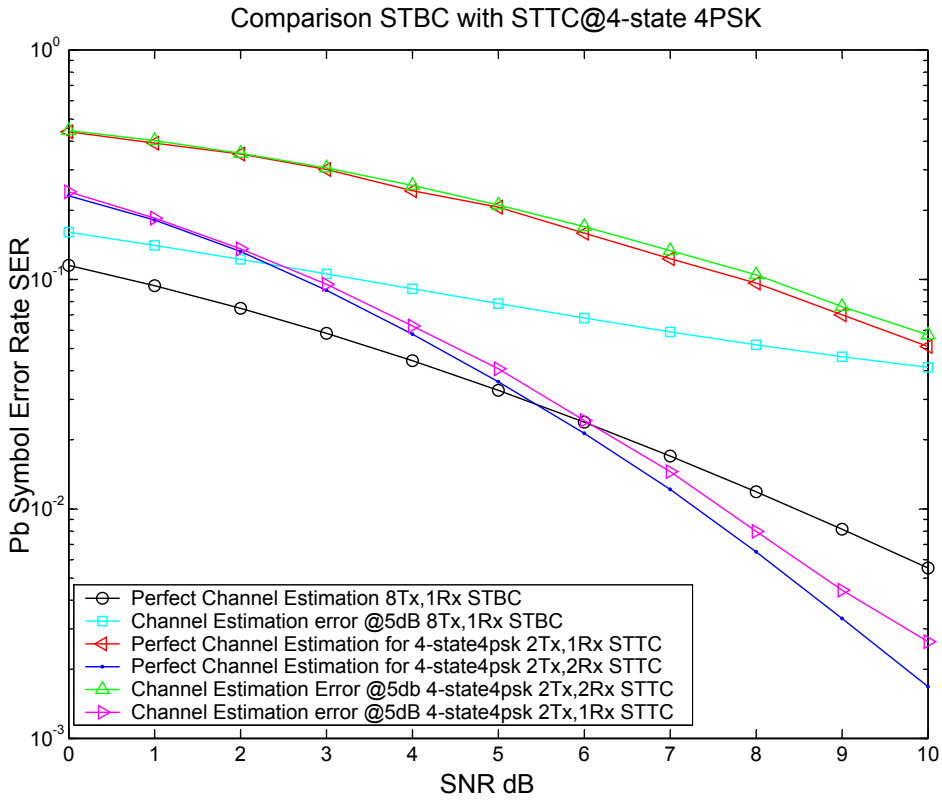

Figure 4.12: Comparison STBC with STTC

4.6 Conclusions

Comparing the results for STTC with those of STBC , it can be concluded that:

1) STTC's performance is better than STBC's in flat slow fading;

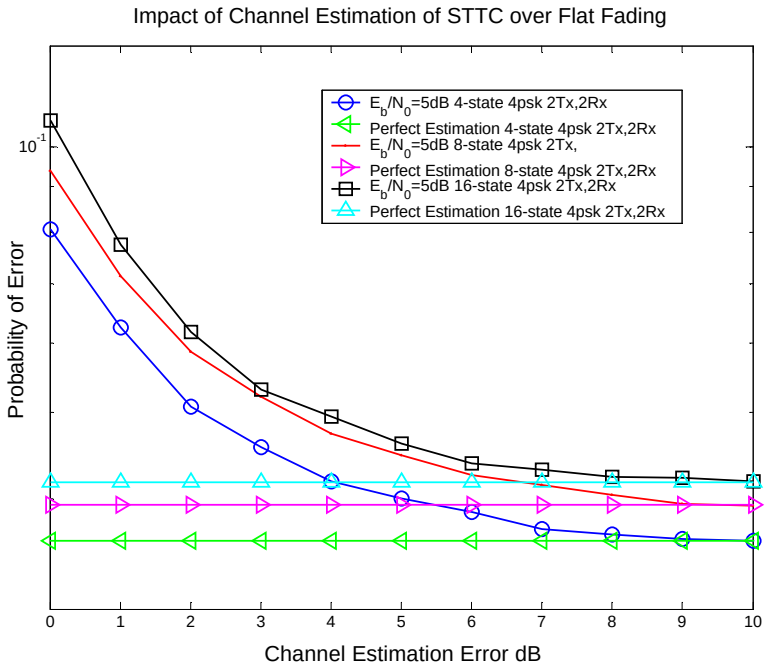

Figure 4.13: Effect of Channel Estimation to STTC

2) STBC is significantly more sensitive to channel estimation error;

3) STTC's structure and implementation is more complex than STBC's. Actually, a better code method has not been found for frequency selective fading for STTC, which is the main obstacle for the applications of STTC in practical systems.

4) Considering the fact that the channel estimation error increases with the number of transmit antennas, if the length of the pilot is fixed, improvements for the channel estimation are necessary to keep the benefits of STBC.

Chapter 5

Conclusions and future work

5.1 Conclusion

In this thesis,a theoretical analysis of the impact of channel estimation error on Space-Time Block and Trellis Codes has been investigated. STBC and STTC represent novel transmission schemes that were originally introduced by a group of researchers from AT&T research labs in an effort to achieve a portion of the capacity growth offered by employing antenna arrays at both ends of the wireless link. The main features of these codes are their holistic design principles, combining entities that were traditionally designed independently (e.g., error correction code, modulation and array processing). This joint design allows STC to achieve the benefits of coded-modulation techniques with full spatial diversity order, and thus offering significant improvements in throughput and link reliability. The schemes

are particularly suited for improving the downlink performance, which is the bottleneck in asymmetric applications such as Internet browsing and downloading.

Channel estimation is an important part of STC. This thesis provides a simple way to measure the impact of channel estimation. The theoretical and simulation results have shown that the impact of channel estimation is important and can be significant. Comparing the performance of STBC to STTC, one can draw the conclusion that STBC is more sensitive than STTC to channel estimation error. Based on this conclusion, the major challenge is to improve the channel estimation scheme if STBC is chosen. Although STTC is more robust and its performance is better than STBC, there are still some problems in implementation. STBC is much easier to implement, but the performance does not improve with the number of antennas if channel estimation error is considered. Thus we must balance performance and complexity. Based upon simulations in this thesis, 4 branch diversity (include 4Tx1Rx or 2Tx2Rx) provide better solutions.

5.2 Future work

This work has shown the significance of the channel estimation error on the performance of STBC and STTC. Future work should compare STBC with channel estimation error with differential Space-Time Block Codes. Future work could also investigate the impact of channel estimation error on quasi-orthogonal block codes.

Bibliography

[1] J.C. Bellamy. *Digital Telephony.* Wiley, New York, 2000.

[2] M. R. Aaron. Digital communications-the silent (r)evolution. *IEEE Communication Magazine*, vol.163:16–26, 1979.

[3] Gordon L. Stuber. *Principles of Mobile communication-Second Edition.* Kluwer Academic Publishers, 2001.

[4] Tero Ojanpera. *Wideband CDMA for Third Generation Mobile Communications.* Artech House Publishers, 1998.

[5] Thedodore S. Rappaport. *Wireless Communications Principles and Practice Second Edition.* Prentice Hall PTR, NJ, 2002.

[6] R. W. Lucky. Automatic equalization for dogital communication. *Bell System Tech.*, vol.44:547–588, 1965.

[7] J. G. Proakis and J. Miler. An adaptive receiver for digital signaling through channels with isi. *IEEE Trans. on Information theory*, IT-15.:484–497, July 1969.

[8] J. Salz R. Lucky and E. Weldon. *Princples of Data Communication.* McGraw-Hill, New York, 1968.

[9] S. U. Qureshi. Adaptive equalization. *IEEE*, vol.73:1349–1387, Sept. 1985.

[10] Khalid Hamied and Gordon L. Stuber. The design of trellis codes for multipath fading isi channel with mlse receivers. *IEEE International Conference*, vol. 1:13–17, May 1994.

[11] N. Seshadri V. Tarokh and A. R. Calderbank. Space-time codes for high data rate wireless communication:performance analysis and code construction. *IEEE Trans. Inform. Theory.*, vol.44:744–765, March, 1998.

[12] G. J. Foschini and M. J. Gans. On limits of wireless communications in a fading environment when using multiple antennas. *Wireless Personal Communications.*, vol.6:311–335, 1998.

[13] S. M. Alamouti. A simple transmit diversity technique for wireless communication. *IEEE J. Select. Area Commun*, vol.16, 1998.

[14] Christian Schlegel and Zachary Bagley. Mimo channels and space-time coding. *Tutorial Presenation, Banff, AB, Canada.*, July, 2002.

[15] Ran Gozali. Space-time codes for high data rate wireless commuincations. *Virginia Tech Dissertation,*, 2002.

[16] W. C. Jakes. *Mobile Microwave Communication.* Wiley, New York, 1974.

[17] H. Jafarkhani V. Tarokh and A. R. Calderbank. Space-time block codes from orthogonal designs. *IEEE Trans. Inform. Theory.*, vol.45:1456–1467, July,1999.

[18] N.A. Kumar and R.M. Buehrer. The impact of channel estimation error on space-time block codes. *Proc. of the Fall 2002 Vehicular Technology Conference, Vancouver Canada*, Sept. 2003.

[19] J. L. Massey. Coding and modulation in digital communications. *Int. Zurich Sem. Digital Communications, Switzerland*, page E2.1.

[20] G. Ungerbock. Channel coding with multilevel phase signals. *IEEE Trans. Inform. Theory.*, vol. 28:55–67, Jan,1982.

[21] P. McLane E. Biglieri, D. Divsalar and M. Simon. *Introduction to Trellis-Coded Modulation with Applications*. McMillan, New York, 1991.

[22] G.D. Forney. The viterbi algorithm. *Proceedings of the IEEE.*, pages 268–278, Mar. 1978.

[23] J. G. Proakis. *Digiatl Communications.* McGraw-Hill, New York, 2000.

[24] Vahid Tarokh. Ayman F. Naguib. A space-time coding modem for high-data-rate wireless communications. *Selected Areas in Communications.*, pages 1459–1477, Oct. 1998.

[25] J.Yuan Z. Chen and B. Vucetic. Improved space-time trellis coded modulation scheme on slow rayleigh fading channel. *IEEE.*, pages 440–441, Mar. 2001.

[26] G. Bauch S. Baro and A. Hansmann. Improved codes for space-time trellis coded modulation. *IEEE com*, vol. 4:20–22, Jan,2000.

Vite

Xuan Chi was born on May 4, 1970, in Anshan, P.R. China. He received his B.S.E.E. degree in electrical and computer engineering from Northeastern University, P.R. China in 1994. From 1994-1999, he was a Engineer at CERIS. (Beijing Central Engineering and Research Incorporation of Iron and Steel Industrial), P.R. China. Currently, Xuan is a Master student at the Mobile and Portable Radio Research Group, Virginia Tech, working in the area of space-time coding with Dr. R. Michael Buehrer. His research interests include Space Time Coding, RF circuit design and RFIC design.